A&A 393, 149–166 (2002)
DOI: 10.1051/0004-6361:20020676

Astronomy & Astrophysics

The modelling of intermediate-age stellar populations

I. Near-infrared properties

M. Mouhcine⋆ and A. Lançon

Observatoire Astronomique, Université L. Pasteur & CNRS: UMR 7550, 11 rue de l'Université, 67000 Strasbourg, France

Received 10 July 2001 / Accepted 25 April 2002

Abstract. Evolutionary population synthesis predictions for stellar systems with complex star formation histories rest on their major building blocks: single-burst population models. In this paper, we discuss how the integrated properties of intermediate-age single-burst populations, especially in the near-infrared, behave as a function of age and metallicity. Our models take into account all stellar evolutionary phases that affect the evolution of the integrated optical and near-infrared spectrum of such a population. Particular care was dedicated to the Asymptotic Giant Branch (AGB) stars, which can be dominant at near-infrared wavelengths. First, we present a new synthetic model that takes into account the relevant physical processes that control the evolution through the thermally pulsing AGB, namely (i) the mass-loss, (ii) the third dredge-up, and (iii) the envelope burning. We use this model to evaluate the AGB-termination luminosity, carbon star properties as function of initial metallicity and initial mass, and the contribution of these stars to the integrated light. In the isochrones presented in this paper the lifetime and the nature of the AGB stars (oxygen-rich or carbon-rich) are established as consequences of the interplay between the physical processes that control the AGB star evolution. The contribution of these stars to the integrated light of the population is thus obtained in a consistent way. We optimize our models by using a new stellar spectral library that explicitly takes into account the spectral features that characterize only AGB stars in comparison to other cool and luminous stars. We analyze the contribution of the upper AGB to the bolometric and the near-infrared light. Our models reproduce the contributions of luminous AGB stars to the bolometric and K-band light, and the carbon star contribution to the bolometric light as observed in the Magellanic Cloud star clusters in a satisfactory way, without ad hoc correction factors that could force agreement. Second, we describe the changes occurring in the integrated colours when AGB stars first appear. We confirm that, in contrast with the classical point of view, no sharp optical/near-infrared colour jump occurs when AGB stars start to dominate the stellar population. The envelope burning process that affects massive AGB stars, making them overluminous with respect to early standard core mass-luminosity relations, causes a smoothing of the colour evolution for stellar systems dominated by those stars. We reanalyze the observational strategy proposed by Lançon et al. (1999) to identify intermediate-age stellar populations in post-starburst spectra using our new model sets. The new spectrophotometric models constitute a first step in a more extended study aimed at modelling the spectral properties of the galaxies in the near-infrared.

Key words. stars: AGB and post-AGB – galaxies: star clusters – galaxies: stellar content – infrared: galaxies

1. Introduction

Evolutionary population synthesis is now a standard tool to investigate the evolution of galaxies in the nearby and distant universe. The observed features of a galaxy, where a mixture of stellar populations of different ages and chemical compositions is present, is modelled by summing spectra of appropriate single-burst populations, which themselves are modelled by summing the contributions of individual stars of the appropriate single age and metallicity (Tinsley 1980; Charlot & Bruzual 1991; Fioc & Rocca-Volmerange 1997; Maraston 1998).

The accuracy of the theoretical predictions of population synthesis models to study the spectrophotometric evolution of galaxies depends on the quality and the completeness of the stellar input physics used to model the set of chemically homogeneous aging single-burst populations. Before facing the problem of modelling observed stellar populations with complex star formation histories, the reliability of the burst population properties as a function of their two fundamental parameters, age and metallicity, needs to be secured. Comparisons of the stellar tracks and derived isochrones with the observed features of stellar clusters, for which the internal spread of stellar ages and metallicities is generally small enough to be consistent with the definition of a burst population, is a necessary preliminary task.

Much effort has been made in recent years to compare properties of synthetic burst populations to the observed features of

Send offprint requests to: M. Mouhcine,
e-mail: mouhcine@astro.ucla.edu
⋆ *Present address:* Departement of Physics & Astronomy, UCLA, Math-Sciences Building 8979, Los Angeles, CA 90095-1562, USA

star clusters (e.g. Arimoto & Bica 1989; Bruzual & Charlot 1993; Girardi et al. 1995). Very good agreement is now commonly found between the observed and the predicted UV and optical properties. This expresses our good understanding of the main-sequence and early giant phases that dominate UV and optical light. Concerning the near-infrared (near-IR), however, many problems remain unsolved and the agreement between the predicted and observed properties is far from being satisfactory. The evolution near-IR colours behaves quite differently from the regular trends found in the evolution of UV/visual colours. The near-IR light is determined by cool and intrinsically luminous late type stars, especially by supergiants (for populations younger than ∼50 Myr), AGB stars (for populations up to ∼1.5–2 Gyr), and Early-AGB (hereafter E-AGB) and red giant branch (hereafter RGB) stars (for old populations). The contribution of those evolutionary phases to the near-IR light varies strongly with age and metallicity, as a consequence of their complex evolution that is controlled by the interplay between different badly-known processes.

In addition to the difficulties directly related to the physics of the evolution of the most luminous red stars, investigations of integrated near-IR properties of intermediate-age stellar populations are hampered by large stochastic fluctuations in available observations, due to the small number of bright AGB stars present in typical star clusters of Local Group galaxies (Santos & Frogel 1997; Lançon & Mouhcine 2000). Until more observations of very massive clusters become accessible, tests of spectrophotometric models remain based on the clusters of the Magellanic Clouds, of which only a few exceed 10^5 $M_\odot$. Agreement with the trends in these data should of course be sought, but it is clear that using them as blind constraints on the evolution of intermediate-age stellar populations holds dangers (see also Marigo et al. 1996b).

In the following, we will focus on evolutionary aspects of AGB stars that may affect their contribution to the integrated properties of a stellar population. Stars with initial masses of $0.9\ M_\odot \leq M_{\rm init} \leq$ 6–8 $M_\odot$ go through a double-shell thermonuclear burning phase, referred to as the Thermally Pulsing AGB (TP-AGB) phase, at the end of their life on the AGB. The double-shell burning is unstable and leads to thermal pulses, that drive quasi-periodic luminosity modulations. In this evolutionary phase, carbon-rich material can be carried up to the envelope by a temporary growth of the convective zone, which is referred to as the third dredge-up. By mixing additional carbon into the envelope a star can be transformed from spectral type K or M (oxygen-rich), to an S-star (C ∼ O), or to a carbon star (carbon outnumbering oxygen). Spectra of oxygen-rich stars are dominated by metal oxide bands such as TiO, VO, and H_2O, whereas carbon stars have bands of C_2 and CN. Carbon stars are known to strongly dominate the near-IR light of intermediate-age globular clusters (Persson et al. 1983; Frogel et al. 1990). The efficiency of the formation of carbon stars as function of age and metallicity is still matter of debate.

Observations of AGB stars in the Galaxy, LMC, and SMC show that the mass-loss rates reached by AGB stars are higher, by orders of magnitude, than those typical of RGB stars. The mass loss is the key process controlling the lifetime of the TP-AGB. The exact processes responsible for such high mass-loss rates are still unknown, but there is a growing amount of evidence from both observational and theoretical points of view, that pulsations coupled with radiation pressure on dust grains play a major role. Hydrodynamical models for Long-Period Variable stars (period of 100−1000 days) show that pulsations may levitate matter to radii where grains form efficiently, so that radiation pressure on dust may then accelerate the gas beyond the escape velocity (Bowen & Wilson 1991). Observationally, well defined correlations exist between the period of pulsation and the mass-loss rates (Schild 1989; Vassiliadis & Wood 1993; see Habing 1996 for comprehensive review).

For the more massive of the AGB stars, significant burning through the CNO cycle can occur at the bottom of the convective envelope, a process referred to as envelope burning (Blöcker & Schönberner 1991; Boothroyd & Sackmann 1992; Vassiliadis & Wood 1993). The immediate result is a breakdown of the core mass-luminosity relations long considered "standard", as those AGB stars become brighter than otherwise expected (see, e.g., Marigo et al. 1999b). The higher luminosity triggers higher mass-loss rates, leading the star to an earlier death. Thus the final core mass attained by these stars is lower than it would be if the stars had obeyed the "standard" core mass-luminosity relation. This effect can prevent an AGB star from becoming a supernova, which has probably had strong consequences on the chemical history of galaxies. The envelope burning delays the formation of carbon stars, since ^{12}C is converted into ^{13}C and ^{14}N, and it gives rise to the formation of ^{13}C-rich stars (usually referred to as J-type carbon stars) and ^{14}N objects (Richer et al. 1979). Theoretical (Boothroyd et al. 1995) and observational (Smith et al. 1995) results suggest that the envelope burning is a common phenomenon, and that virtually all AGB stars brighter than $M_{\rm bol} = -6$ undergo envelope burning.

In this paper, we address the theoretical behaviour of the integrated colours, focusing on the near-IR properties of intermediate-age stellar populations dominated by AGB stars, with the aim of illustrating and updating our knowledge about the contribution of AGB stars to these properties. Our further goal is to improve the diagnostic power of near-IR spectra of galaxies, to retrieve information about the ages and metallicities of their stellar populations. After a brief statement about background considerations we consider fundamental (Sect. 2), Sect. 3 presents the grid of stellar evolutionary tracks constructed to calculate theoretical isochrones. They include all evolutionary phases from the main-sequence to the end of the AGB phase. Particular attention is paid to the TP-AGB, which is included by means of a synthetic model including all relevant physical processes known to control the evolutionary properties that will finally affect integrated stellar population properties. In Sect. 4 we present the evolution of near-IR properties of intermediate-age stellar populations (i.e., contributions of AGB stars to the integrated light, broad-band colours, and narrow-band colours). We discuss how they depend on age and metallicity. Comparisons with observations in the Magellanic Clouds are shown and discussed. Photometric indices that may help detecting intermediate-age populations in integrated light are re-visited. Finally, in Sect. 5 our conclusions are drawn.

2. Theoretical background

The concept of *fuel consumption* is useful to draw first conclusions about the evolution of integrated properties of single-burst populations as a function of time, and to become aware of the precautions needed when constructing self-consistent models. As pointed out by different authors (Renzini & Buzzoni 1986; Girardi & Bertelli 1998), a relation exists between the bolometric luminosity of an evolving burst population and the final mass of its current turn-off stars. This is due to two facts: (i) the lifetime in post-main sequence phases is very short in comparison to the main sequence lifetime, and (ii) the luminosity emitted in each post-main sequence phase is related to the core mass growth during this phase. If we consider, in addition, a monotonic relation between the initial mass and the total lifetime, we can expect that the evolution of the bolometric luminosity of the stellar population will just reflect the initial-to-final mass relation. Such considerations are also important because the final core mass at envelope ejection has direct implications for the integrated UV light of old stellar populations (Chiosi et al. 1997).

When modelling the spectrophotometric evolution of stellar populations, it is fundamental to reproduce the basic observational constraint of the initial-to-final mass relation before facing other observational constraints relative to the integrated properties. As intermediate-mass stars lose a large part of their mass during the TP-AGB phase, a preliminary task is to model the history of mass loss along the AGB phase. Detailed modelling of the near-infrared properties requires, moreover, an accurate representation of the spectral properties of AGB stars, as the latter emit the bulk of their energy in this range of the spectrum. The two tasks are related since stars with massive final cores are, in general, the coolest and the more luminous of the stars present.

In this paper we will focus on the evolutionary aspects of the AGB, while the average spectra of oxygen-rich and carbon-rich TP-AGB stars used in our spectrophotometric calculations are discussed in a companion paper (Lançon & Mouhcine 2002; hereafter Paper II).

3. Evolutionary tracks and AGB evolution

In this section we present the evolutionary tracks used to compute the integrated properties of intermediate-age stellar populations.

3.1. Up to the end of Early-AGB

The stellar evolutionary tracks from the main sequence and up to the Early-AGB (E-AGB hereafter) phase used in our calculations are those of Bressan et al. (1994a) and Fagotto et al. (1994), for [$Z = 0.008$, $Y = 0.25$] and [$Z = 0.02$, $Y = 0.28$]. The reader is referred to those papers for more details. We note that a convective overshooting scheme was adopted in these calculations, lowering the values of the limiting initial masses for building degenerate C–O cores after the exhaustion of central helium.

3.2. Synthetic evolution of TP-AGB stars

Full calculations of the evolution of the structure and appearance of TP-AGB stars are still computationaly expensive, and only restricted grids in initial mass and metallicity can be found in the literature. In this context, synthetic evolution models provide an attractive tool to study evolutionary and chemical properties of TP-AGB stars (Iben & Truran 1978; Renzini & Voli 1981; Iben & Renzini 1983; Groenewegen & de Jong 1993; Marigo et al. 1996a). Synthetic models are based on analytical representations of the results of full numerical calculations; they explicitly include the physical processes that most directly affect the evolution along the TP-AGB, and make it possible to test their respective effects.

We follow the TP-AGB evolution in a synthetic way, starting from the last E-AGB models from the adopted tracks. The total mass M, the core mass $M_{\rm c}$, the effective temperature $T_{\rm eff}$, the luminosity L, the mass loss rate, and the carbon to oxygen ratio of the models are left to evolve according to analytical formulae that inter-relate these quantities and their time derivatives. The equations are based on the prescriptions of Wagenhuber & Groenewegen (1998, hereafter WG98), and on previous work by Groenewegen & de Jong (1993), and Vassiliadis & Wood (1993). The prescriptions of WG98 are a high accuracy reproduction of the results from extensive grids of complete evolutionary calculations carried out by Wagenhuber (1996) for stars in the range $0.8\ M_{\odot} \leq M \leq 7\ M_{\odot}$ and metallicities $Z = 10^{-4}$, $Z = 0.008$ and $Z = 0.02$.

3.2.1. Thermal pulses of AGB stars

Fundamental relations in synthetic AGB models are the core mass – luminosity relation, which gives the maximum luminosity during the quiescent hydrogen burning episodes, and the core mass – interpulse period relation, which gives the time separation between two successive thermal pulses (Paczyński 1970; Iben & Truran 1978; Boothroyd & Sackmann 1988a; Blöcker 1995). Predictions of TP-AGB evolution are significantly influenced by these input prescriptions: the luminosity affects the mass-loss rates, and the interpulse period affects the evolution of the chemical abundance of the envelope, and hence the spectral properties of those stars.

The maximum bolometric luminosity during the quiescent hydrogen burning is written as a sum expressing the contributions of different processes (WG98):

$$L = 18160 + 3980\log(Z/Z_{\odot})(M_{\rm c} - 0.4468) \quad (1a)$$
$$+10^{2.705+1.649M_{\rm c}} \quad (1b)$$
$$\times 10^{0.0237(\alpha-1.447)M_{\rm c,0}^2 M_{\rm env}^2(1-\exp(-\Delta M_{\rm c}/0.1))} \quad (1c)$$
$$-10^{3.529-(M_{\rm c,o}-0.4468)\Delta M_{\rm c}/0.01} \quad (1d)$$

Z denotes the initial metallicity, $M_{\rm c,0}$ is the core mass at the first thermal pulse, $\Delta M_{\rm c}$ is the core mass growth since the beginning of the TP-AGB (i.e. $\Delta M_{\rm c} = M_{\rm c} - M_{\rm c,0}$), and $M_{\rm env}$ is the current envelope mass. Masses and luminosities are expressed in solar units. This core mass-luminosity relation has the advantage of including relevant physical processes that were omitted in early versions. The first term expresses the usual linear relation

in the full amplitude regime of the thermal pulses (Paczyński 1975; Vassiliadis & Wood 1993); the second term provides a correction that becomes significant for high core mass stars ($M_c \geq 0.95\,M_\odot$); the third term accounts for the excess of luminosity produced by envelope burning, which drops when the envelope mass is reduced; the last term provides a correction for the "turn-on" effects, i.e. the progressive growth of the thermal pulses early on the TP-AGB. This formulation gives us the opportunity to look into the effect of the envelope burning, of the convective mixing length α and of the chemical composition on the integrated properties. Our *standard model* will use $\alpha = 2$ (Blöcker & Schönberner 1991).

The core mass – interpulse period relation is given by:

$$\begin{aligned}\log \tau_{\rm ip} \;=\; & (-3.628 + 0.1337 \log(Z/Z_\odot))(M_c - 1.9454) \\ & -10^{-2.080-0.353\log(Z/Z_\odot)+0.2(M_{\rm env}+\alpha-1.5)} \\ & -10^{-0.626-70.30(M_{c,o}-\log(Z/Z_\odot))\Delta M_c}. \end{aligned} \quad (2)$$

Again, the first term expresses the standard relation, a decreasing function of the core mass with some dependence on the metallicity. The second term accounts for envelope burning, by somewhat reducing this time interval. The final term corrects for the progressive turn-on of the pulses before the asymptotic regime is reached. The influence of the initial metallicity on the interpulse period is strong, in the sense that the interpulse period increases with decreasing metallicity.

Between two thermal pulses, the luminosity is not constant. The helium flashes drive deviations from the luminosity given by the core mass – luminosity relation. Those variations have a strong effect on the AGB star populations, in particular on the bright tail of the AGB luminosity function (Marigo et al. 1996a). We use the prescriptions of WG98 to calculate the interpulse light curves.

To obtain the position of a star in the HR diagram and to calculate the mass loss rate, an estimate of the stellar effective temperature is needed. We use the analytical relation presented by Wagenhuber (1996). This relation is based on stellar models with carbon-to-oxygen number ratios below one. We use it even when stars become carbon-rich, although carbon star atmospheres are expected to be more compact than those of M type stars (Scholz & Tsuji 1984; Loidl et al. 2001). A complete integration of the envelope and atmosphere equations with abundance dependent opacities would provide more consistent positions in the *theoretical* HR diagram, but our purpose is to predict *observable* properties. Fundamental uncertainties related to the definition of the effective temperature of AGB stars and its relation to observable properties (e.g. the available spectra) are discussed in detail by Baschek et al. (1991) and in Paper II. These uncertainties are large, and justify an a posteriori calibration of the relation between the effective temperature of TP-AGB stars and their colours in any case. Therefore, the theoretical absolute effective temperature scale of the TP-AGB tracks is not critical.

3.2.2. Mass loss rates

One of the most important processes controlling the secular evolution of AGB stars in the HR diagram and their spectral type is the mass loss rate (Bedijn 1987; Bryan et al. 1990; Blöcker 1995; Frost et al. 1998; Zijlstra 1999). It affects the lifetime and the average luminosity of stars in this phase. Both these quantities shape the contribution of the whole phase to the integrated light. The larger the mass-loss rate, the shorter is the lifetime of the TP-AGB phase, the dimmer are its brightest stars (at wavelengths sensitive to circumstellar obscuration), and the lower is the contribution to the total light of the population. In addition, a high mass loss rate favours the formation of carbon stars, since less carbon needs to be dredged up to change the carbon-to-oxygen abundance ratio of a less massive envelope. Unfortunately, mass-loss is still poorly understood. The mass loss dependence on the fundamental stellar parameters and the mass loss efficiency η are still far from being definitively determined. Unless otherwise stated, we will use the analytical mass loss prescription of Blöcker (1995), derived from the hydrodynamical models for Long Period Variable stars (LPVs) of Bowen (1988):

$$\dot{M} = 4.83\ 10^{-9}\,\eta\,L^{2.7}\,M^{-2.1}\,\dot{M}_{\rm R} \quad (3)$$

where η is the mass loss efficiency and $\dot{M}_{\rm R}$ is Reimers's mass loss rate (i.e., $\dot{M}_{\rm R} = 1.27 \times 10^{-5}\,\eta_{\rm R} M^{-1} L^{1.5} T_{\rm eff}^{-2}$, with $\eta_{\rm R} = 1$). This formulation of the mass loss is particularly sensitive to the luminosity. In our *standard model* a value of $\eta = 0.1$ will be used as suggested by Groenewegen et al. (1994) from fitting the luminosity function of carbon stars in the LMC. In stars with relatively high initial masses, the strong decrease of the current mass along the TP-AGB contributes to producing the observed superwinds, that terminate this evolutionary phase. The effect of the effective temperature on the evolution of $\dot{M}$ at a given metallicity is smaller. The average $T_{\rm eff}$ of the evolutionary tracks however depends on metallicity, which contributes to lowering the mass loss of metal deficient stars. We do not consider an explicit metallicity dependence in the mass loss rate.

3.2.3. The rate of evolution

Hydrogen burning is the dominant source of energy during most of the interpulse period. The equation that describes the core growth in $M_\odot\ {\rm yr}^{-1}$ reads:

$$\frac{{\rm d}M_c}{{\rm d}t} = q(Z)\frac{L_{\rm H}}{X} \quad (4)$$

where $q(Z)$, the mass burnt per unit energy release is slightly metallicity dependent, X is the hydrogen abundance by mass in the envelope, and $L_{\rm H}$ the luminosity provided by the burning of hydrogen. Since there is some contribution to the total energy from the core shrinking and helium burning, the luminosity produced by the hydrogen burning that enters Eq. (4) is smaller than the total luminosity derived from the core mass-luminosity relation, so that (WG98):

$$\log\left(\frac{L_{\rm H}}{L}\right) = -0.012 - 10^{-1.25-113\Delta M_c} - 0.0016 M_{\rm env}. \quad (5)$$

Here L is is the luminosity derived using the core mass-luminosity relation, with the term providing a correction for the envelope burning (e.g. Eq. (1c)) set to unity.

3.2.4. Chemical evolution of TP-AGB stars

Between the main sequence turn-off and the tip of the AGB phase, low to intermediate-mass stars experience three types of dredge-up episodes, during which material that underwent nuclear burning is mixed to the surface by envelope convection. During the first dredge-up episode, where the star reaches its Hayashi track after the hydrogen exhaustion in the core, and the second dredge-up at the base of the E-AGB, products from the CNO cycle are transported to the surface; third dredge-up episodes during the TP-AGB bring up helium shell burning products as well. In our calculations, the chemical abundances prior to the onset of the third dredge-up during the TP-AGB phase are directly taken from the evolutionary tracks used for the evolutionary phases earlier than the TP-AGB phase.

The third dredge-up plays a crucial role in the formation of carbon stars as it leads to the enrichment of the surface in carbon. As most convection-determined phenomena, dredge-up is not yet fully understood. The amount of ^{12}C enhancement increases strongly with the metallicity and mass (Wood 1981; Lattanzio 1987; Boothroyd & Sackmann 1988b; Vassiliadis & Wood 1993). Most stellar evolution calculations fail to predict carbon stars at luminosities as low as observed, and are only able to obtain dredge-up for relatively high initial stellar masses ($M \geq 1.5\,M_{\odot}$; e.g. Blöcker 1995; Forestini & Charbonnel 1997; Wagenhuber & Weiss 1994). Boothroyd & Sackmann (1988b) were able to find dredge-up in a 0.81 $M_{\odot}$ and $Z = 10^{-3}$ star, but using a very high mixing length parameter (i.e. $\alpha = 3$), which is questionable. There is still much debate whether or not material is dredged up at every thermal pulse, and how much (Blöcker 1999; Mowlavi 1999). The observed carbon stars luminosity function requires that the dredge-up occurs efficiently to produce carbon stars for initial masses of about $\sim$1.3$-$1.4 $M_{\odot}$ (Groenewegen et al. 1995; Marigo et al. 1996a).

The semi-analytical treatment of the third dredge-up process used in this paper requires three basic inputs: (i) the critical core mass $M_{\rm c}^{\rm min}$ above which it is assumed that dredge-up occurs (we relax the condition that the thermal pulse must have reached the full amplitude regime, introduced as an assumption by Groenewegen & de Jong 1993), (ii) the dredge-up efficiency parameter, defined as the fraction of the core mass growth that will be dredged up to the envelope ($\lambda = \Delta M_{\rm dredge}/\Delta M_{\rm c}$, where $\Delta M_{\rm c} = \int_0^{\tau_{\rm ip}} ({\rm d}M_{\rm c}/{\rm d}t){\rm d}t$), and (iii) the composition of the material in the convective inter-shell after a thermal pulse and before the penetration of the convective envelope; this is the material that will be dredged-up, mainly consisting of helium, carbon, and oxygen. We have adopted $M_{\rm c}^{\rm min} = 0.58\,M_{\odot}$ and $\lambda = 0.75$, as required to reproduce the luminosity function of field carbon stars in the LMC (Groenewegen & de Jong 1993; see also Marigo et al. 1996a, 1999a), and the chemical composition of the convective inter-shell is taken from Boothroyd & Sackmann (1988a).

The second effect which can heavily alter the surface chemical composition of TP-AGB stars is envelope burning. This effect prevents or delays the conversion to carbon stars for massive AGB stars, because of the efficient burning of carbon-rich dredged-up material to nitrogen. The physical conditions needed to trigger this process, and its efficiency, are still uncertain. To take envelope burning into account, we procede as follows. We assume that envelope burning is effective (e.g. that CNO cycle is operating at the base of the envelope), for sufficiently luminous stars ($\log(L/L_{\odot}) \gtrsim 4.2$), only if the envelope mass exceeds a certain value $M_{\rm env}^{\rm EB}$ (see Marigo 1998, for an alternative approach). As an estimate of this critical value, we use the approximation derived by WG98:

$$M_{\rm env}^{\rm EB} = M(1 - 0.2\alpha - 5Z) \tag{6}$$

where $M_{\rm env}^{\rm EB}$ and M are, respectively, the current envelope mass and total mass. α is the mixing length parameter, and Z is the stellar initial metallicity. Within the framework of our semi-analytical treatment, dredge-up can occur even after envelope burning has stopped near the end of the TP-AGB. This is of vital importance to reproduce the formation of observed luminous carbon stars (van Loon et al. 1998; Frost et al. 1998; Mouhcine & Lançon 2002).

Denoting by $X_i^{\rm new}$, $X_i^{\rm shell}$ the abundance of the element i in the envelope and in the inter-shell, by $M_{\rm env}$ the mass of the envelope just before the pulse, and by $\Delta M_{\rm dup}$ the mass dredged up to the envelope after the pulse, the new surface abundance after the pulse is written:

$$X_i^{\rm new} = \frac{X_i^{\rm old} M_{\rm env} + X_i^{\rm shell} \Delta M_{\rm dup}}{M_{\rm env} + \Delta M_{\rm dup}} + \Delta X_i^{\rm EB}. \tag{7}$$

The second term in the right side of Eq. (7) takes into account the abundance variation due to envelope burning. To calculate the amount of the dredged up material and the envelope material that undergo thermonuclear burning at the bottom of the envelope, we follow the semi-analytical approach adopted by Groenewegen & de Jong (1993), based on the results of Renzini & Voli (1981). In order to calculate the time evolution of the chemical abundances, we use the approach presented by Clayton (1983). The basic assumption in this method is that the two reaction chains of the CNO-cycle (i.e., the CN-cycle and the ON-cycle) can be separated. The nuclear reaction rates are taken from Fowler et al. (1975).

3.3. The end of the AGB evolution

The TP-AGB phase ends with the total ejection of the envelope, when the star moves from the red to the blue side of the HR diagram. In practice, we follow a star's evolution until the envelope mass is reduced below 10% of the core mass growth during the last interpulse period (Iben 1985). The TP-AGB evolution is also stopped when the core mass reaches the Chandrasekhar limit ($\sim$1.4 $M_{\odot}$) just before carbon deflagration would occur. In our models however, this condition is never met, being prevented under the influence of the stellar mass loss.

3.4. Results and constraints

For the purpose of this paper, we have restricted the computation of the semi-analytical TP-AGB star evolution to two initial metallicities, [$Z = 0.008$, $Y = 0.25$] and [$Z = 0.02$, $Y = 0.28$]. Each set of tracks covers the initial mass range of 0.9 $M_{\odot}$$-$$M_{\rm up}$.

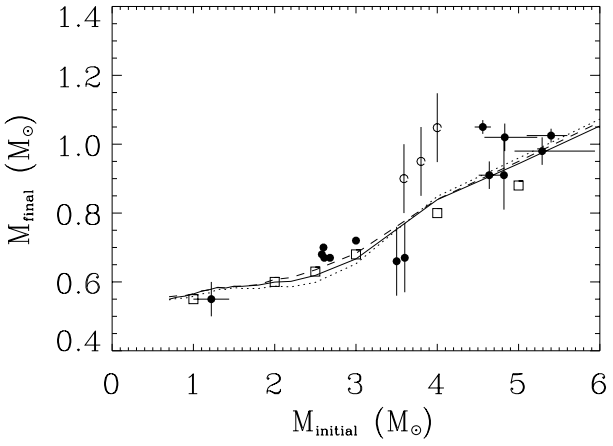

Fig. 1. Final stellar remnant mass after complete ejection of the envelope, plotted as a function of the initial mass for solar metallicity models, for three mass-loss prescriptions: Blöcker (1993, continuous line), Reimers (1975, dotted line), Vassiliadis & Wood (1993, long-dashed line). $\alpha = 2$ is assumed. Observational data are taken from Jeffries (1997), Herwig (1995), Weidemann (2000, open squares). Open points with error bars represent data points of lower quality (cf. Herwig 1995).

M_{up} is taken equal to 5 $M_\odot$ for $Z = 0.008$, and equal to 6 $M_\odot$ for $Z = 0.02$. In the following subsection, we present and discuss the evolution of the properties of TP-AGB stars that are relevant to the purpose of this paper.

Complete grids of evolutionary tracks and isochrones for an extended metallicity grid (from $Z/Z_\odot = 1/50$ to $Z/Z_\odot = 2.5$) have been computed, and are being used to interpret carbon star counts in galaxies (Mouhcine & Lançon 2002). They will be published elsewhere (in preparation).

3.4.1. The initial-final mass relation

In Fig. 1 the final core mass, M_{final}, left after the complete ejection of the envelope is plotted against the initial mass M_{init} of each model for solar metallicity. The predicted initial-final mass relations for both metallicities considered in this paper ($Z = 0.02$ and $Z = 0.008$) are tabulated in Table 1, together with the maximum quiescent bolometric luminosity reached on the TP-AGB, the total lifetime of the TP-AGB phase, and the fraction of this duration spent as a carbon star. The final mass can be considered as the mass of the remnant white dwarf.

The theoretical predictions of Fig. 1 are computed using different mass-loss prescriptions, based on those of Blöcker (1995), but also those of Reimers (1975) and Vassiliadis & Wood (1993). We have modified the mass loss prescriptions using calibrated mass-loss efficiencies (Groenewegen & de Jong 1994; Marigo et al. 1996a). Also shown in the plot is the semi-empirical initial-final mass relation from Herwig (1995), Jeffries (1997), and the new revisited relation from Weidemann (2000) for the solar neighbourhood. Very good agreement is seen between the predicted solar metallicity initial-final relation and the most recent semi-empirical determination. This agreement shows that the effects of the envelope burning and the third dredge-up are important in determining the evolution of the stellar core mass along the TP-AGB (and hence the contribution of AGB stars to the integrated light of stellar populations). Indeed, the reduction of the core mass by recurrent third dredge-up events keeps the core mass close to its value at the begining of the TP-AGB phase. Neglecting these effects, as in some previous population synthesis models that take into account a simplified TP-AGB phase, leads to the prediction of much higher final masses than observed (see for example Bertelli et al. 1994; Girardi et al. 2000). The net effect of the choice of one or the other mass-loss prescription, in comparison, is small.

Table 1. For $Z = 0.02$ and $Z = 0.008$ and for each initial mass M_{init} (in $M_\odot$), the table lists the values of the final mass M_{final}, the brightest quiescent bolometric magnitude M_{bol}, the lifetime on the TP-AGB τ_{TP-AGB} (in Myr), and the fraction of the TP-AGB lifetime spent as a carbon star. The predicted values are those of our standard model ($\alpha = 2$, $\eta = 0.1$, and $\lambda = 0.75$).

Z_{init}	M_{init}	M_{final}	M_{bol}	τ_{TP-AGB}	τ_c/τ_{TP-AGB}
0.02	0.931	0.549	–3.952	0.175	0.000
	1.000	0.556	–4.058	0.282	0.000
	1.078	0.559	–4.161	0.423	0.000
	1.159	0.565	–4.291	0.481	0.000
	1.242	0.573	–4.393	0.508	0.000
	1.328	0.578	–4.469	0.588	0.000
	1.413	0.584	–4.554	0.555	0.000
	1.499	0.582	–4.561	0.731	0.076
	1.585	0.587	–4.594	0.791	0.083
	1.670	0.587	–4.657	0.986	0.139
	1.840	0.591	–4.729	1.398	0.110
	2.016	0.599	–4.799	1.591	0.329
	2.200	0.602	–4.867	2.125	0.286
	2.500	0.619	–4.989	2.402	0.518
	3.000	0.667	–5.331	1.503	0.455
	4.000	0.839	–6.025	1.438	0.000
	5.000	0.943	–6.309	0.060	0.0015
	6.000	1.053	–6.715	0.022	0.000
0.008	0.899	0.544	–3.942	0.365	0.000
	0.949	0.549	–3.960	0.393	0.000
	1.062	0.56	–4.175	0.518	0.000
	1.230	0.573	–4.460	0.726	0.000
	1.404	0.581	–4.641	0.859	0.097
	1.576	0.583	–4.717	1.065	0.158
	1.748	0.588	–4.772	1.531	0.296
	2.000	0.596	–4.862	2.333	0.298
	2.500	0.623	–5.101	2.781	0.779
	3.000	0.685	–5.498	1.127	0.768
	4.000	0.899	–6.22	0.0676	0.00
	5.000	0.977	–6.432	0.0449	0.00

3.4.2. TP-AGB lifetimes

The contribution of TP-AGB stars to the integrated properties of a stellar population depends on the time stars spend on the TP-AGB. The lifetime of this phase is mainly determined by the mass-loss history, and essentially by the onset of the superwind, and it depends in a complex way both on stellar mass and on metallicity (Vassiliadis & Wood 1993).

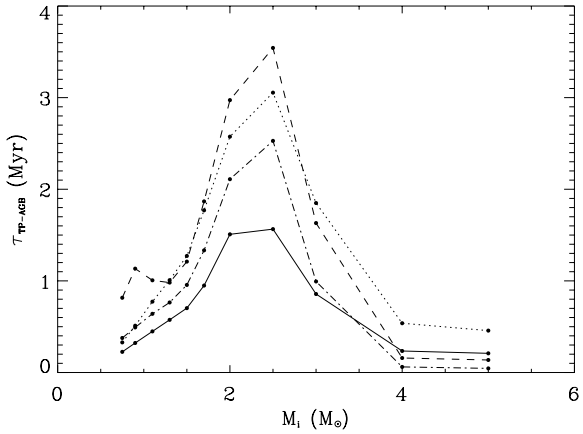

Fig. 2. Theoretical total TP-AGB lifetime as a function of initial mass for LMC metallicity. Different mass loss prescriptions were used: Reimers' law (1975; solid line), Blöcker's prescription (1993; dashed), Vassiliadis & Wood (1993; dot-dashed), Baud & Habing (1983; dotted).

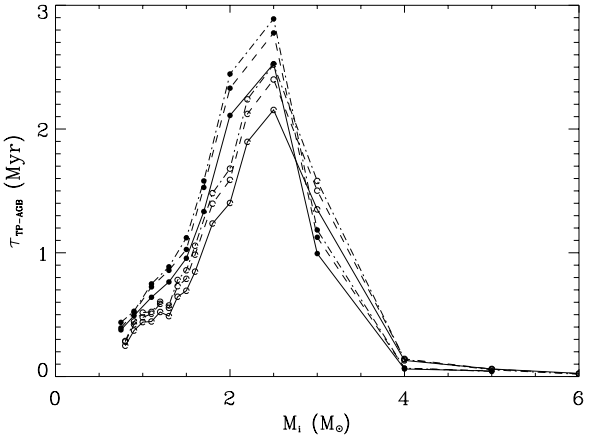

Fig. 3. Total TP-AGB lifetime as a function of initial mass. Filled and open circles correspond, respectively, to LMC and solar metallicities. Different mixing length parameters were used in the calculations: α = 1.5 (continuous line), α = 2 (dashed line), and α = 2.5 (dot-dashed line).

Figure 2 shows the evolution of the TP-AGB lifetime as a function of initial mass for the metallicity of the LMC, using different mass loss prescriptions as indicated in the caption. The plot shows that, for any given mass-loss prescription, the TP-AGB phase is an increasing function of stellar mass in the low mass range ($M_i \leq 2.5\ M_\odot$), while for higher masses the trend is the opposite. The figure clearly shows how sensitive the TP-AGB lifetimes are to the adopted mass-loss prescription.

Note that while the initial-final mass relation does not show a strong dependence on calibrated mass-loss prescriptions, the lifetime of the TP-AGB phase does. The initial-final mass relation does not tell us how how rapidly material is burnt during the TP-AGB phase. These considerations are of great interest for population synthesis models of resolved stellar populations (Mouhcine & Lançon 2002).

Figure 3 compares the evolution of the TP-AGB phase lifetime as a function of initial mass for solar and LMC metallicities. The plot shows that the total TP-AGB lifetime

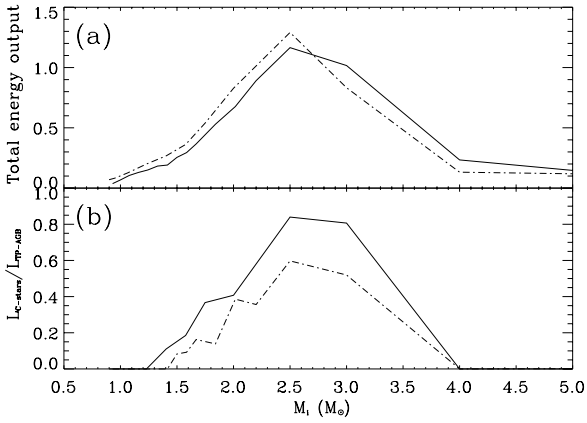

Fig. 4. a) Total amount of energy (in units of $10^4\ L_\odot$ Myr) produced during the TP-AGB phase for LMC (solid line) and solar (dashed line) metallicities, as predicted by our standard models (η = 0.1, α = 2, λ = 0.75). **b)** Corresponding fraction of the total energy emitted by the TP-AGB stars while they are carbon-rich stars.

increases with decreasing metallicity. This is due to the fact that low-metallicity stars have globally warmer asymptotic giant branches and need to evolve to higher luminosities in order to reach the superwind regime and to end their TP-AGB lives. Raising the value of the mixing length parameter increases the relative lifetime of the TP-AGB phase. This is related to the fact that increasing α produces warmer effective temperatures, making the phase lifetime longer. However, the quantitative dependence on α remains small. The derived average lifetime of luminous, massive TP-AGB stars ($M_{\rm init} \gtrsim 3.5$–$4\ M_\odot$, $-7 \lesssim M_{\rm bol} \lesssim -6$, mean period of variability 500–900 days) is of the order of a few 10^5 yr, which is consistent with the observational constraints (Reid et al. 1990; Hughes & Wood 1990; see Sect. 3.4.3). At both metallicities, maximal TP-AGB lifetime is obtained for stars with initial masses of 2–$2.5\ M_\odot$, which evolve off the main sequence several 10^8 yrs after they were born.

Related to the total lifetime of the TP-AGB phase is the total amount of energy emitted during this phase, which is closely related to the so-called fuel consumption. Figure 4 shows the total TP-AGB energy output and the fraction of this output produced by carbon stars (Sect. 3.4.4), for the two metallicities investigated.

3.4.3. Pulsating stars on the AGB

While evolving along the AGB phase, stars may, for at least part of their lifetime, undergo large amplitude, long period pulsations (period of 100−1000 days). This evolutionary feature applies to the two classes of LPVs, namely the optically visible Miras and semi-regular variables, with low or moderate mass-loss rates, and the dust-enshrouded OH/IR or "C/IR" stars (carbon-rich infrared sources), with high mass-loss rates (Wood et al. 1992, 1998; Wood 1998).

Coupled with a period-mass-radius relation (Wood 1990), the present model predicts the period range that LPVs on the TP-AGB may have. Figure 5 illustrates the results at the metallicity of the LMC. For each mass, it shows the bolometric magnitude $M_{\rm bol}$ as a function of pulsation period, for the evolutionary points just prior to the occurrence of each thermal pulse

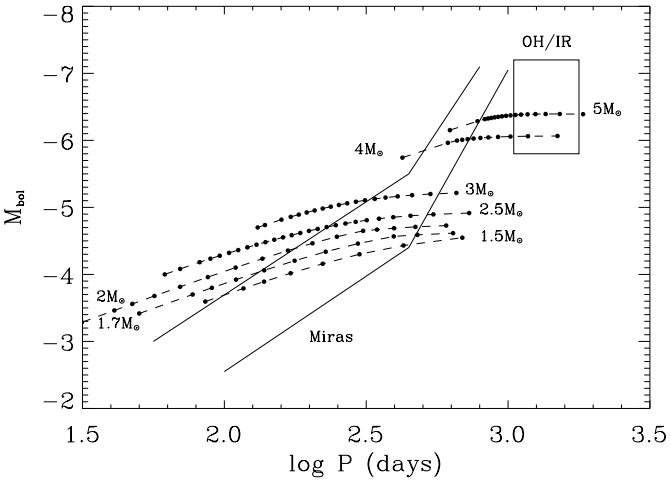

Fig. 5. The fundamental mode period – luminosity relations for stars with initial chemical composition [Z = 0.008, Y = 0.25] and our standard model parameters. Initial masses are indicated. The observed P-L relation for optically visible LPVs in the LMC is delineated by the two full lines from Hughes & Wood (1990). Also shown is the observed location of dust-enshrouded oxygen-rich AGB (OH/IR) stars from Wood et al. (1992). The evolutionary points plotted here correspond to the maximum luminosity during the quiescent hydrogen burning phase of the helium flash cycles.

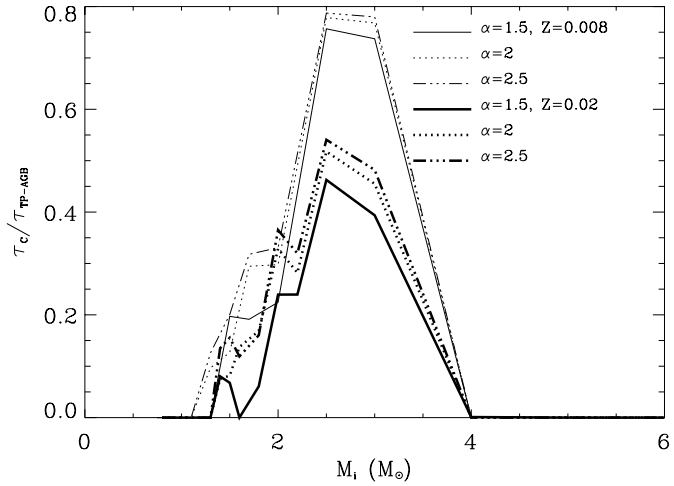

Fig. 6. Fraction of the TP-AGB lifetime spent as a carbon star, for solar metallicity and LMC metallicity, assuming different mixing length parameters as indicated. The mass loss prescription from Blöcker (1995) was used with $\eta = 0.1$.

assuming that LPV pulsation occurs during the entire TP-AGB phase. For all masses the first point shown corresponds to the first thermal pulse on the TP-AGB, while successive points on the tracks are separated by one interpulse period. We assumed that LPVs are fundamental mode pulsators, which is now considered appropriate for Miras (Wood et al. 1999). When exactly LPV pulsation starts on the TP-AGB, and when the transitions from overtone pulsation to lower orders and finally to fundamental mode pulsation occur, is presently unknown because the necessary non-linear pulsation models of these complex cool stars are rare and uncertain (Barthès & Luri 2001 and references therein). Initially, the stars evolve up the AGB increasing in luminosity and period until the onset of the superwind regime, at which point the period quickly grows to higher values. The acceleration to longer period is more dramatic for massive stars. This is because there is more mass to lose, and because the period strongly depends on both the mass and the effective temperature. Among massive stars ($M_{\rm init} \gtrsim 3\ M_{\odot}$), the final period is an increasing fonction of initial mass.

We show in Fig. 5 the zone occupied by optically visible LPVs (Hughes & Wood 1990) and dust-enshrouded stars (Wood et al. 1992), as observed in the LMC. The agreement with the predictions is satisfactory. We note that for $M_{\rm init} \lesssim 2.5{-}3\ M_{\odot}$ the tracks are essentially located in the region occupied by the optically visible variable stars, before the onset of a brief superwind phase. More massive tracks evolve rapidly from the location of optically visible variables to the location of stars in the superwind regime. This may indicate that only relatively massive AGB stars (i.e., $M_{\rm init} \geq 3.5{-}4\ M_{\odot}$) are able to evolve as heavily dust-enshrouded objects. The low luminosity zone of the observed Period-Magnitude relation where there are no evolutionary tracks can be explained by low-mass stars in the luminosity dip that follows a thermal pulse.

3.4.4. Carbon stars

One of the main goals of this paper is to introduce carbon stars into spectrophotometric models in a self-consistent way. Using our TP-AGB synthetic evolution models, we thus investigate the formation of carbon stars. Here we present some properties of these carbon stars that allow us to understand their effects on integrated near-infrared properties and the sensitivity of the latter to the metallicity. The distribution and the effects of carbon stars on the stellar population properties depends on the lifetime of stars in the carbon-rich phase. This lifetime depends primarily on the initial mass and metallicity.

In Fig. 6 we plot the theoretical fraction of the total TP-AGB lifetime that a star spends as a carbon star, versus the initial mass, for the two metallicities considered in this paper and different choices of the mixing length parameter. The plot shows clearly that the production of carbon stars is a function of both the metallicity and the initial stellar mass. In an instantaneous burst scenario, the carbon star subpopulation will thus depend on the age of its parent population. The striking features are: (i) at a given metallicity, the relative lifetime of the carbon-rich phase is an increasing function of stellar mass in the low mass range ($M \lesssim 2.5{-}3\ M_{\odot}$), while for higher masses the trend is reversed, and (ii) at a given initial mass the relative lifetime of the carbon-rich phase is significantly larger for models with lower metallicity. This behaviour is consistent with observational findings (see Mouhcine & Lançon 2002 for references and discussion). In the initial mass range most favourable to the formation of carbon stars, a rise of the value of the mixing length parameter increases the TP-AGB lifetime without significantly changing the time it takes a star to become carbon-rich. The carbon star lifetime relative to the TP-AGB lifetime thus increases. However, the increase remains small if compared to the effect of metallicity.

It is noteworthy that $\tau_{\rm C}/\tau_{\rm TP-AGB}$ is largest for initial masses that also have the longest TP-AGB lifetime. This is clearly demonstrated by the effect of the mixing length parameter

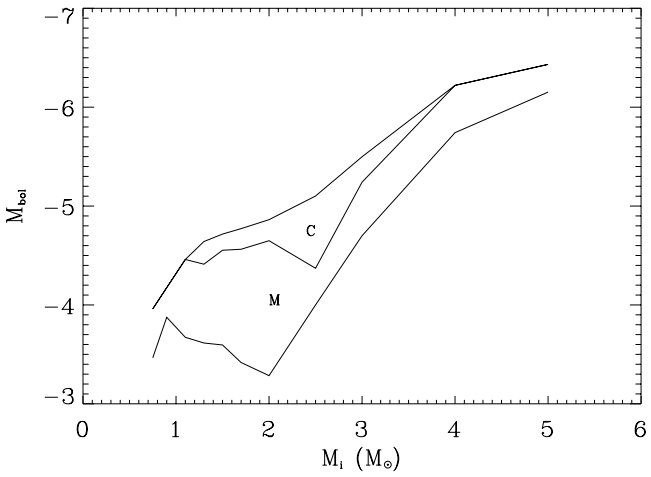

Fig. 7. Bolometric magnitude of important transitions for TP-AGB stars with initial metallicity $Z = 0.008$. Shown are the transitions from the E-AGB to the TP-AGB (lowest line), the transition from spectral type M to spectral type C (intermediate line), and the end of the TP-AGB (top line), as functions of initial mass.

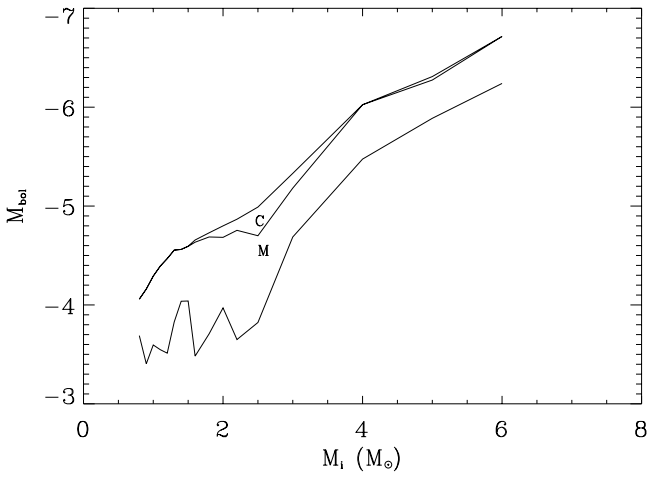

Fig. 8. Same as Fig. 7, but for the initial metallicity $Z = 0.02$.

α on the evolution of τ_C/τ_{TP-AGB}. Increasing α, increases τ_C/τ_{TP-AGB} similarily to its effect on τ_{TP-AGB}. The longest relative lifetimes as carbon stars indeed correspond to the longest absolute lifetime of the carbon-rich phase.

Another way of illustrating the role of carbon stars is to look at the integrated bolometric luminosity emitted during this phase. Figure 4b shows the predicted fraction of the total amount of TP-AGB fuel burnt during the carbon-rich phase versus the initial mass of the stars. The features of these curves are qualitatively similar to those noted for the time fraction that TP-AGB stars spend as carbon-rich objects. This directly follows from the fact that the integrated energy emitted by any evolutionary phase scales with the lifetime and with the average luminosity of this phase. Along an evolutionary track, the average luminosity of the carbon stars is only slightly higher than that of the oxygen-rich TP-AGB stars, and hence the ratio of energy outputs is only slightly higher than τ_c/τ_{TP-AGB}. The figure foreshadows that the contribution of carbon stars to the integrated properties of stellar populations will be maximum when the turn-off mass is $M_{TO} \approx 2.5\ M_\odot$.

Figures 7 and 8 show the bolometric magnitude M_{bol} at which stars with various initial masses (M_{init}) reach the TP-AGB, become carbon stars, and leave the TP-AGB. The three boundary lines delimit two areas in the $M_{bol}-M_{init}$ diagram: the region marked "M" corresponds to the locus of TP-AGB stars of spectral type M (or K; with C/O < 1); the region marked "C" represents the domain occupied by the carbon stars (defined as stars having C/O ≥ 1). Note that the luminosities plotted are quiescent luminosities, and that the flash-driven light curves will temporarily move stars of a given type outside the delineated areas. Two features arise from these plots. The first one is that the bolometric magnitude at the tip of the TP-AGB phase is strongly dependent on the metallicity as well as on the initial mass of the star: the lower the metallicity, the more luminous is the tip of the AGB for a given initial mass (see also Marigo et al. 1996a). One needs to keep this property in mind when attempting to derive constraints on the age of stellar populations: the high end of the luminosity function of TP-AGB stars is sensitive to metallicity. The second feature concerns the dips in the M-to-C transition curves around $M_{init} = 2.5\ M_\odot$. The dip is more pronounced at LMC metallicity than at solar metallicity. Note that the prefered initial mass range for the formation of carbon stars is similar for solar and LMC metallicities in the $M_{bol}-M_{init}$ diagram.

3.5. The stellar spectral library

Theoretical and empirical stellar libraries are becoming more and more reliable, and have now included most evolutionary phases of stellar evolution. However, none of the stellar libraries commonly used for the evolutionary synthesis of stellar population spectra (e.g. Lejeune et al. 1998; Pickles 1998) accounts for the specific spectral properties of luminous AGB stars. Previous attempts to model intermediate-age populations use static giant star spectra to model the spectral energy distribution even of LPVs on the asymptotic giant branch. However, the library of spectra of luminous red stars of Lançon & Wood (2000) has confirmed that those stars have spectra quite different from those of static M giants. For instance, their near-IR spectra display stronger molecular absorption bands than static giant star spectra, as a consequence of pulsations that make these stars more extended and cooler than static ones (Bessell et al. 1989). In addition, no previous evolutionary synthesis predictions explicitly include spectra of carbon stars (only broad band colours of these objects have sometimes been used). In this paper, we use the spectra of Lançon & Wood (2000) for static luminous red stars, the average spectra of Paper II for oxygen rich and carbon rich LPVs, and the library of Lejeune et al. (1998) in all other cases. We assume that early-AGB stars are static, and TP-AGB stars variable. The reader is referred to Paper II for a discussion.

4. Evolution of integrated properties

In this section, we use the TP-AGB evolutionary tracks described above to investigate the near-IR properties of single-burst populations. As discussed, we now have at our disposal

the following essential elements of such calculations and of their interpretation:

1. The location of TP-AGB stars in the HR diagram as a function of initial mass and initial metallicity;
2. the total lifetime of the TP-AGB phase;
3. the age marking the transition from M star class (C/O < 1) to carbon star class (C/O ≥ 1);
4. a spectral library including oxygen-rich and carbon-rich TP-AGB stars.

In the following, we will present the contribution of AGB stars to the integrated light and the evolution of integrated optical/near-IR colours. In all our synthetic populations, stars are distributed at birth according to the initial mass function (IMF) of Salpeter (1955; $\phi(m) \propto m^{-2.35}$).

4.1. Fractional contribution of AGB stars to the total luminosity

Analyzing the contribution of AGB stars to bolometric light is instructive in the sense that it tells us when those stars are important in the energy budget of a population. The temporal evolution of the contribution of the AGB stars to the bolometric light essentially reflects the evolution of the AGB lifetime as function of the initial mass (i.e. Fig. 2). This is illustrated in Fig. 9. Instead of the contribution of the TP-AGB stars stricto sensu the contribution of stars brighter than $M_{\rm bol} = -3.6$ is shown, in order to allow for direct comparison with existing observations (Figs. 7 and 8 show that this limit is close to the actual TP-AGB limit at most relevant ages).

The data represent the fractional bolometric luminosities accounted for by such stars in clusters of various ages in the Magellanic Clouds (Frogel et al. 1990). AGB stars are intrinsically rare objects. In intermediate-age star clusters such as those of the Magellanic Clouds, with masses of the order of 10^5 $M_\odot$ or smaller, the number of luminous AGB stars varies between a small handful and about 20. The number and luminosity of AGB stars are subject to stochastic fluctuations from one cluster to another one of similar age, and therefore so are the AGB contributions to the integrated light (Ferraro et al. 1995; Girardi et al. 1995; Santos & Frogel 1997; Lançon & Mouhcine 2000). To limit this effect, the 39 clusters of the Frogel et al. (1990) sample have been grouped into age bins. The error bars on the luminosity contribution in Fig. 9 represent the rms dispersion of these data at $1\,\sigma$, but do not include membership uncertainties. Using the clusters common to the two samples, we determined the linear transformation from the SWB class given by Frogel et al. (1990; see Searle et al. 1980) to the S parameter redefined by Girardi et al. (1995). Then the cluster ages were assigned using the relation of Girardi et al. (1995) between the S parameter and age: $\log(t/\mathrm{yrs}) = 0.0733 \times S + 6.227$. This relation is based on the same evolutionary models as ours (up to the TP-AGB; the latter however has insignificant impact on the optical colours characterizing SWB classes).

Figure 9 shows that our model predictions reproduce the variations of the contribution of the AGB stars with age. The contribution of AGB stars increases gradually from a few

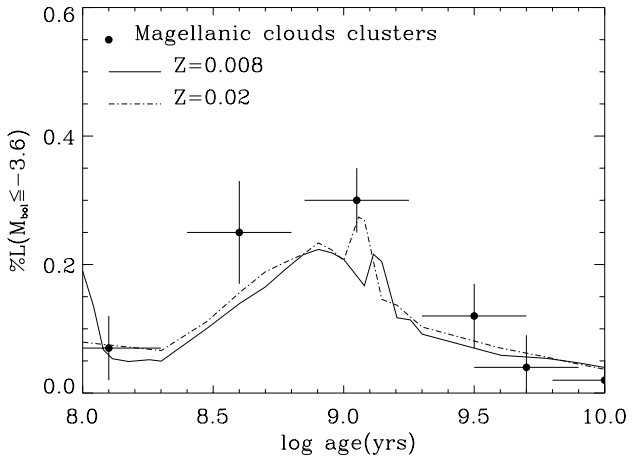

Fig. 9. The predicted fractional bolometric luminosity of single stellar populations that arises from AGB stars, as a function of time, for the metallicities indicated. LMC cluster data are adapted from Frogel et al. (1990) using the age calibration of Girardi et al. (1995). Error bars indicate $1\,\sigma$ uncertainties due to small number statistics, but neglect membership uncertainties in the samples.

percent at 0.1–0.2 Gyr (between SWB type 3 and 5) up to ∼25% at 0.5–1 Gyr. This behaviour is due to the effect of envelope burning on massive AGB stars, which reduces their lifetime and hence their total emitted light. In models without envelope burning, the maximum contribution of AGB stars occurs at younger ages. The peak in the AGB contribution is located at the age when the turn-off stars have the largest TP-AGB lifetime. Our peak values are compatible with the data in view of the many empirical uncertainties. Nevertheless, they lie slightly below the observed mean: the important effects of AGB stars on the integrated spectrum, discussed in following sections, are not overestimates. For populations older than ∼1 Gyr, the contribution of AGB stars decreases with increasing age as a consequence of shorter lifetimes and smaller individual luminosities. Note that TP-AGB stars dominate the contribution of AGB stars to the bolometric light, and account for more than 80% of the total AGB luminosity at ∼1 Gyr.

Figure 9 shows that the contribution of bright AGB stars to the bolometric light is not very sensitive to the metallicity in the range explored here. This is mainly because the core mass and the envelope mass at the start of the TP-AGB phase do not strongly depend on initial stellar metallicity. The sharp and short increase of the contribution of AGB stars that takes place at $\log(\mathrm{age}) \approx 9.15$ is due to the first emergence of AGB stars that have degenerate helium cores during their RGB phase (see Sect. 4.3 and Fig. 5 of Girardi & Bertelli 1998).

Figure 10 shows the evolution of the contribution of carbon stars to the integrated bolometric luminosity of a single-burst population for $Z = 0.008$ and $Z = 0.02$. Overplotted are the empirical fractional bolometric luminosities of carbon stars as observed in Magellanic Clouds clusters (Frogel et al. 1990). The horizontal error bars refer to the age interval covered by the considered SWB types. Similarly to the total AGB contribution, the fractional contribution of carbon stars is shaped by the evolution of the lifetime in the carbon-rich phase as a

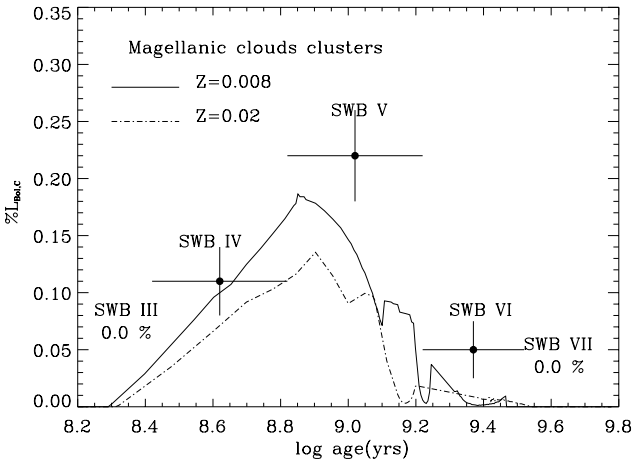

Fig. 10. The fractional bolometric luminosity of single stellar populations that arises from carbon stars, as a function of time, for LMC (continuous line) and solar metallicity (dashed-dotted line). LMC cluster data are adapted from Frogel et al. (1990), as in Fig. 9. The lower the metallicity, the higher the contribution of carbon stars. The maximum contribution corresponds to the age at which stars with the turn-off mass have the longest carbon rich phase.

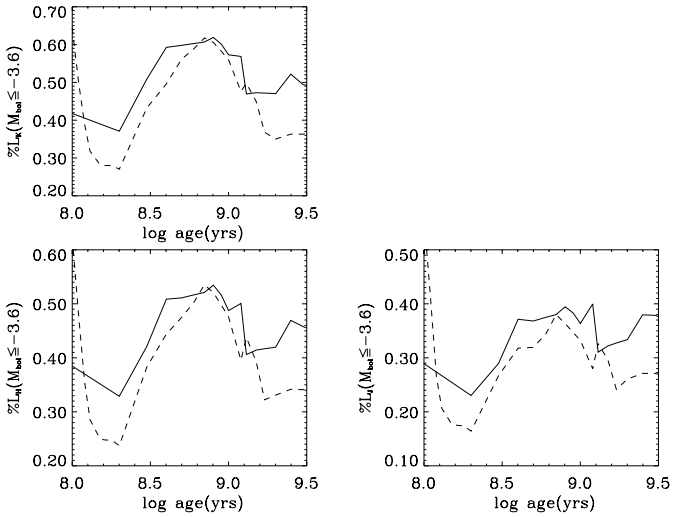

Fig. 11. The fractional near-IR luminosities of single stellar populations that arises from luminous AGB stars as a function of time for $Z = 0.02$ (continuous line) and $Z = 0.008$ (dashed line). The redder the pass-band and the higher the metallicity, the higher is the contribution of TP-AGB stars.

function of initial mass and initial metallicity (Fig. 6). Comparison with Fig. 9 shows that, when present, carbon stars account for a large fraction of the bolometric luminosity from the AGB stars. The models show that carbon stars are present only for stellar populations older than ∼0.2 Gyr, between SWB type 3 and 4 (corresponding to a turn-off mass $M_{\rm TO} \lesssim 4\ M_{\odot}$ with very weak dependence on initial metallicity). This is consistent with the observational constraints from the Magellanic Cloud clusters. The figure shows also that carbon stars appear earlier in metal-poor systems than in metal-rich systems, reflecting both the high efficiency of carbon star formation at low metallicity and the dependence of the total lifetime on metallicity. Then, the contribution of carbon stars increases with age, with a maximum of ∼20% at age of ∼0.8 Gyr. As pointed out for the contribution of luminous AGB stars, at this age the turn-off stars have the largest carbon-rich lifetime. For older systems (age $\gtrsim$ 0.8 Gyr), the contribution of carbon stars decreases with age.

The plot shows that, as expected, the fractional contribution of carbon stars depends strongly on the metallicity. Lower initial metallicity leads to higher contributions of carbon stars to the bolometric light. However, the age when the contribution of carbon stars is maximum is relatively independent of the initial stellar population metallicity, reflecting that the prefered mass range for the formation of carbon stars is the same for both metallicities.

Comparison of the model predictions with the observed data and the conclusions one may draw from this exercise again require caution. The carbon star samples are small and the dispersion in the data large. Again, the plotted uncertainties are rms deviations that do not account for the many uncertain membership (see Table 1 of Frogel et al. 1990). As an example, the LMC clusters NGC 2209 and NGC 269 have the same SWB classification (i.e. the same age), but show completely different contributions from carbon stars. Carbon stars are responsible for 58% of the bolometric light of the first cluster, while they do not contribute at all to the integrated light of the second cluster. More powerful constraints on the formation of carbon stars, and their contribution to integrated light of stellar populations, can be derived using the observed statistics of late-type stellar contents of the fields of resolved galaxies in the local universe, for which the problem of the small number statistics of bright carbon stars is avoided. The evolution of the mean bolometric magnitude of carbon stars in the Local Group galaxies is of particular interest for our purpose. However, in order to use galaxy field stars one needs to disentangle the stellar evolution effects from those of the star formation and the chemical evolution of galaxies. Our results for Local Group galaxies are discussed elsewhere (Mouhcine & Lançon 2002).

In summary, the predicted shape of the temporal evolution of carbon star contributions to the bolometric light is consistent with observations in clusters and constraints from galaxy fields. The age interval during which carbon stars are important contributors to the bolometric light is well matched. This is taken as evidence that the evolution of the carbon-rich phase lifetime as a function of initial mass and metallicity is satisfactorily determined by our models.

4.2. The contributions of AGB stars to near-IR light

In addition to the above, a fundamental and global test for our single stellar population models and for the underlying stellar evolution models, is the comparison of the predicted luminosity contributions to different near-IR bands with measurements in clusters. Analyzing these contributions is important because it provides additional information on the spectral features to be expected in the integrated spectrum in various wavebands.

In Fig. 11 we show, for the two metallicities considered here, the evolving contributions of luminous AGB stars to the integrated light in the J, H and K wavebands. The plot shows that the evolution of the AGB contributions to near-IR light is

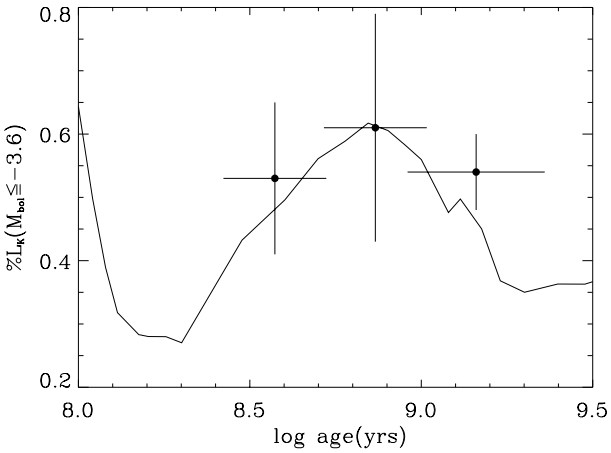

Fig. 12. The AGB contribution to the total K band luminosity compared with globular cluster data from Ferraro et al. (1995). The solid line represents the predicted contribution of AGB stars to the K band luminosity for single stellar population of LMC metallicity. Error bars indicate the rms dispersion in the data.

qualitatively similar to that of their contribution to bolometric light, and that it is controlled again mainly by the evolution of the AGB lifetime with initial mass. The contribution of AGB stars to integrated near-IR light evolves rapidly, for LMC metallicity for example, from a few percent at ∼0.1 Gyr to being the dominant source of the infrared light at ages of ∼0.6–0.7 Gyr, where the contributions vary from ∼40% in the J band to ∼65% in the K band. The plot shows that the contribution of AGB stars increases with increasing metallicity and increasing wavelength. This is because (i) AGB stars are the coolest stars of the population and radiate preferentially in the infrared, and (ii) the average temperature of AGB stars is sensitive to metallicity (higher metallicity lowers the effective temperature of the evolutionary tracks).

In Fig. 12 we show a comparison between the temporal evolution of the AGB contribution to the integrated K band luminosity, as theoretically predicted for $Z = 0.008$ and as observed in a sample of intermediate-age LMC clusters (Ferraro et al. 1995). Unfortunately no observational constraints are available on the contribution of AGB stars to the J band nor the H band luminosities. Globular cluster ages and error bars are as noted above for the contribution of AGB stars to the bolometric light. The plot shows a good agreement between the observed and the predicted K band contributions of the AGB stars. The agreement suggests that the combination of the predicted position of TP-AGB stars on the theoretical HR diagram and their total lifetime is adequately determined by our stellar evolution models.

4.3. The time evolution of integrated colours

We now discuss how the integrated colours evolve in time. We recall that for single-burst populations older than 0.1 Gyr, the near-IR colours depend weakly on the assumed IMF (Maraston 1998).

Figure 13 illustrates the spectral evolution of a solar metallicity, instantaneous burst population between 0.2 and 1 Gyr. The synthetic spectra are constructed using isochrones assembled by means of the evolutionary tracks of Sect. 3 and the stellar library presented in Sect. 3.5. The figure shows the spectral features that characterize the near-IR spectra of intermediate-age populations. The time evolution of the H band spectral energy distribution and of the break-like feature in the J band clearly show the effect of the dominant AGB population. For stellar populations younger than ∼300 Myr, the latter is oxygen-rich, and the near-IR spectra are characterized by features that originate from late type M stars. The H band has a bump-like curved shape (due to the minimum in the continuous H^- opacity and to the wings of water absorption bands), and the J band shows VO absorption at ∼1.05 μm. For older populations, the H band flattens and the ∼1.77 μm break due to C_2 deepens. The water band cut-off around 1.32 μm is progressively hidden in carbon star features and replaced with a CN bandhead at 1.35 μm. Another CN bandhead becomes conspicuous at ∼1.08 μm.

Figure 14 shows the time evolution of the optical/near-IR synthetic broad-band colours for the age interval in which AGB stars are significant. The integrated $VJHK$ magnitudes of the burst populations are obtained by convolving the spectra with the response functions of standard passbands (Bessell 1990; Bessell & Brett 1988). Zero colours are adopted for a model spectrum of Vega (Dreiling & Bell 1980, kindly provided by M. Bessell). The figure illustrates clearly that the presence of AGB stars does not *immediately* translate into a sharp jump of the stellar population colours to the red, but that this transition is gradual over several hundred Myr. This predicted evolution is in contradiction with the classical view of the evolution of optical/near-IR broad-band colours (see e.g. Renzini & Buzzoni 1986; Charlot & Bruzual 1991; Bressan et al. 1994b; Tantalo et al. 1996; Fioc & Rocca-Volmerange 1997), as already noted by Girardi & Bertelli (1998). The predicted behaviour is due to (i) the severe reduction of the TP-AGB phase lifetime of massive stars, and hence the reduction of their contribution to the near-IR integrated light (ii) the absence of a clear transition between the stars affected by the envelope burning and those that follow the standard core mass-luminosity relation. We note that this behaviour is similar for both metallicities considered. The luminosity excess with respect to original core mass-luminosity relations for massive AGB stars causes a temporal smoothing of the colour jumps associated with the appearance of AGB stars.

The impact of AGB stars on the integrated properties of intermediate-age stellar populations is more evident in purely near-IR colours. $(V-K)$ increases as the stellar population ages, even at times when the AGB contribution to K band light decreases, due to the gradual fading of the turn-off stars that dominate the V-band light and the accumulation of large numbers of red giant branch stars that will finally dominate the near-IR light. The purely near-IR colours, on the other hand, increase up to the age of ∼0.8 Gyr, but decrease gradually for older systems up to an age of ∼1.5−2 Gyr. Populations in this age range are likely to explain the *IR enhanced clusters* as defined by Persson et al. (1983). The near-IR colours result directly from the large contribution of AGB stars to the near-IR light, between ages of ∼0.3 and ∼1.5 Gyr. For older systems,

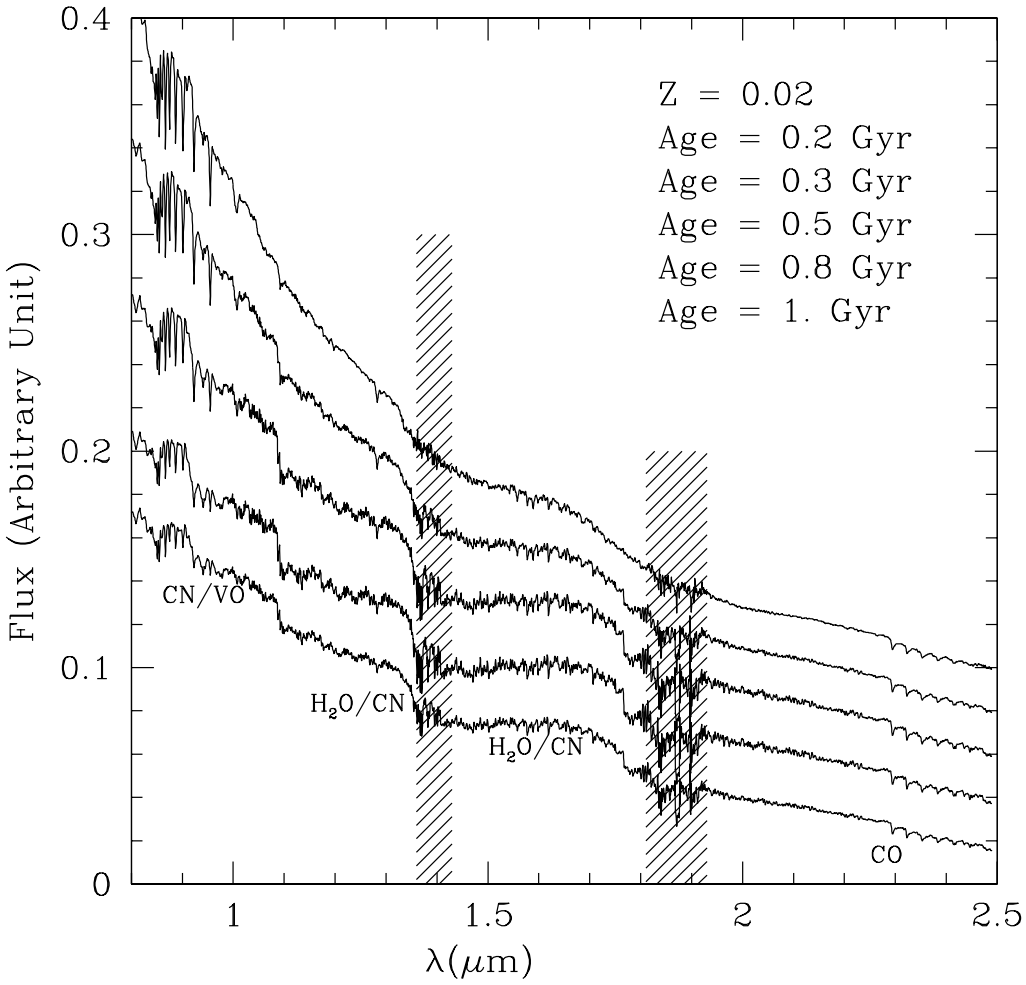

Fig. 13. Evolution of the spectra of instantaneous burst stellar populations as predicted for $Z = 0.02$ for the ages given. Main molecular contributors to the features that characterize the NIR spectra are indicated. They characterize intermediate-age populations and may be used to identify AGB populations. Note particularly the evolution of the H band shape as function of age and the break-like feature at 1.1 μm. Shaded areas are those that could not be corrected for telluric absorption in a satisfactory way.

the AGB stars are not the main contributors and the time evolution reflects the well-known accumulation of red giants. This picture of the optical/near-IR colour evolution is consistent with the evolution of these colours observed in the Magellanic Cloud clusters as a function of SWB type (Fig. 2 in Persson et al. 1983).

An interesting feature of Fig. 14 is that the near-IR colours evolve more rapidly at $Z = 0.008$ than with $Z = 0.02$ models, during the age interval where AGB stars are dominant. This follows from the chemical nature of the predominant AGB populations. Carbon stars are intrinsically redder than oxygen-rich AGBs in colours involving the J band. As pointed out above, carbon stars completely dominate intermediate-age AGB populations at low metallicity, explaining the very red near-IR colours.

Figure 14 shows that there is a brief excursion to red colours, just after the age when turn-off stars have an initial mass equal to the limit for the development of a degenerate helium core. As discussed by Girardi & Bertelli (1998), this transient jump is a feature of the evolutionary models, due to the fact that the core helium burning phase lifetime reduces strongly for stars having an initial mass in the vicinity of the transition mass between stars with and without degenerate helium cores.

To further illustrate the effect of carbon stars on the integrated light, we have computed additional model sequences in which the formation of carbon stars is neglected, and exclusively spectra of oxygen-rich stars are used. Figure 15 shows the differences between synthetic broad-band colours predicted by models that differentiate carbon stars and oxygen-rich stars and models that don't. As expected, (i) near-IR colours calculated including the two AGB subtypes are systematicaly redder than models neglecting the formation of carbon stars, (ii) the changes in the colours between both model sets increase with decreasing metallicity, and (iii) $(V - K)$ is not affected significantly by the nature of dominant AGB population. The models show that neglecting carbon stars has a sizeable effect on the evolution of spectral energy distribution. We find that the effects on the J band are significant, while those on the H and K bands are relatively small. Good near-IR photometry including the J band may be able to tell us if the AGB populations are dominated by carbon stars or not, while $V - K$ is not a useful

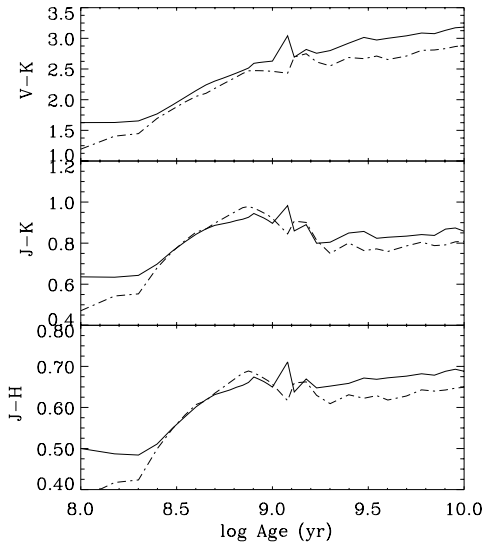

Fig. 14. The time evolution of synthetic broad-band near-IR colours for $Z = 0.02$ (continuous line) and $Z = 0.008$ (dashed-dotted line). The solar models are redder than the LMC metallicity models apart for intermediate-age populations where carbon stars are present. For these systems, $Z = 0.008$ models evolve more rapidly to the red than $Z = 0.02$ models. This behaviour is due to the higher contribution of carbon stars to the integrated light in metal-poor systems.

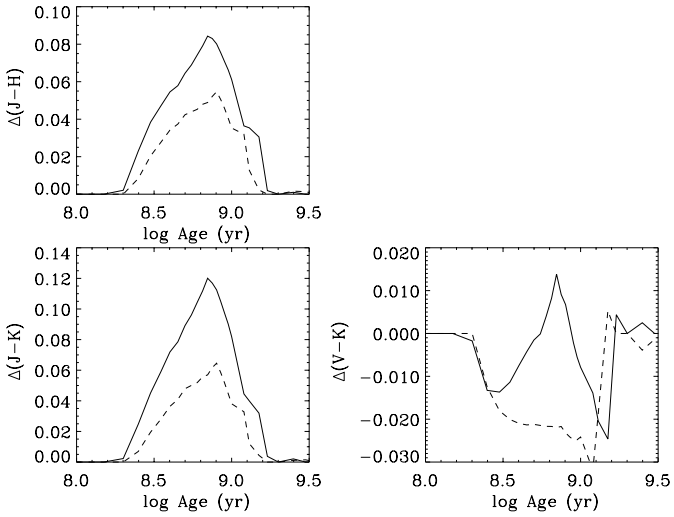

Fig. 15. Differences between the synthetic broad-band colours of models that differentiate carbon stars and oxygen-rich stars and models that neglect the formation of carbon stars, for $Z = 0.008$ (continuous line) and $Z = 0.02$ (dashed-line).

colour for that purpose. As an example, the change in $(J - K)$ between both models, for LMC metallicity at the age when the AGB contribution is largest (age ≈ 0.8 Gyr), is $\Delta(J-K) \approx 0.12$, which is easily observable with the current instrumentation.

Figure 16 shows comparisons between our synthetic colour-colour diagram for stellar populations older than 0.1 Gyr, and observed diagrams for a sample of LMC and SMC globular clusters with available infrared photometry and SWB types older than 3 (Persson et al. 1983). Observational determinations of the age-metallicity relation of Magellanic globular clusters (Olszewski et al. 1991; Da Costa & Hatzidimitriou 1998), show that old clusters have approximately $-1.5 >$ [Fe/H] > -2.2, while young and intermediate-age ones have $0.0 >$ [Fe/H] > -0.6. The significant dispersion of the observed colours, due to the small number of bright and red stars, unfortunately limits the power of the comparisons (Lançon & Mouhcine 2000; Bruzual 2002). We report in the colour-colour diagrams the location of the IR enhanced clusters as defined observationally by Persson et al. (1983). The models show that this regions is occupied by stellar populations with age $8.5 \lesssim \log(t/\mathrm{yr}) \lesssim 9.2$ and, hence, dominated by carbon stars. This is consistent with the data, showing that (i) almost all of these clusters are of intermediate-age, (i.e., in SWB groups IV – VI), and (ii) many members of the IR enhanced cluster group contain identified carbon stars, which help accounting for their red integrated colours.

4.4. Searching for AGB stars in post-starbursts

AGB stars have proven to be powerful tracers of intermediate-age stellar populations in nearby resolved galaxies, and hence tools to infer constraints on the formation history of these galaxies. To retrieve information about relatively recent star formation in unresolved galaxies, Lançon et al. (1999) suggested to use the near-IR signatures of AGB stars present in the integrated spectra. They selected a set of intermediate band filters (among the filters available on the NICMOS camera on board the Hubble Space Telescope), well suited for measurements of the specific LPV features, and appropriate both for the global identification of TP-AGB stars and for the determination of their chemical nature. In this section, we re-evaluate the temporal evolution of such a set of photometric molecular indices.

In the following we will use three indices defined as follows: H_2O ($2\,\mu$m) = F190N1/F215N2, H_2O ($1.64\,\mu$m) = $2 \times$ F190N1/(F164N1 + F215N2), and H_2O/C_2 ($1.77\,\mu$m) = F180M2/F171M2. The passbands of the selected filters are those of the HST/NICMOS filters. All indices are flux ratios (flux in a molecular band divided by an estimate of the flux outside the molecular band), expressed in magnitudes, and they take the value zero for Vega.

Figure 17 shows the resulting two-index diagnostic diagram. High molecular indices unambiguously identify the predominance of AGB stars in single stellar populations. The plot shows that the "IR enhanced" stellar populations, defined as above, also have the most pronounced molecular features. In complex stellar populations, the identification of intermediate-age post-starburst components will depend on the extent of dilution in continuum contributions of either a few red supergiants or many old red giants. Using two molecular indices jointly should allow us to constrain the chemical nature of the dominant AGB subtype, once it has been shown that AGB stars are present: here, the $1.77\ \mu$m H_2O/C_2 index takes systematically higher values for populations with higher fractions of carbon stars.

As already mentioned, the predictions of near-IR spectrophotometric properties of intermediate-age stellar populations requires the use of an effective temperature – colour (or spectrum) calibration for AGB stars. We have constructed two

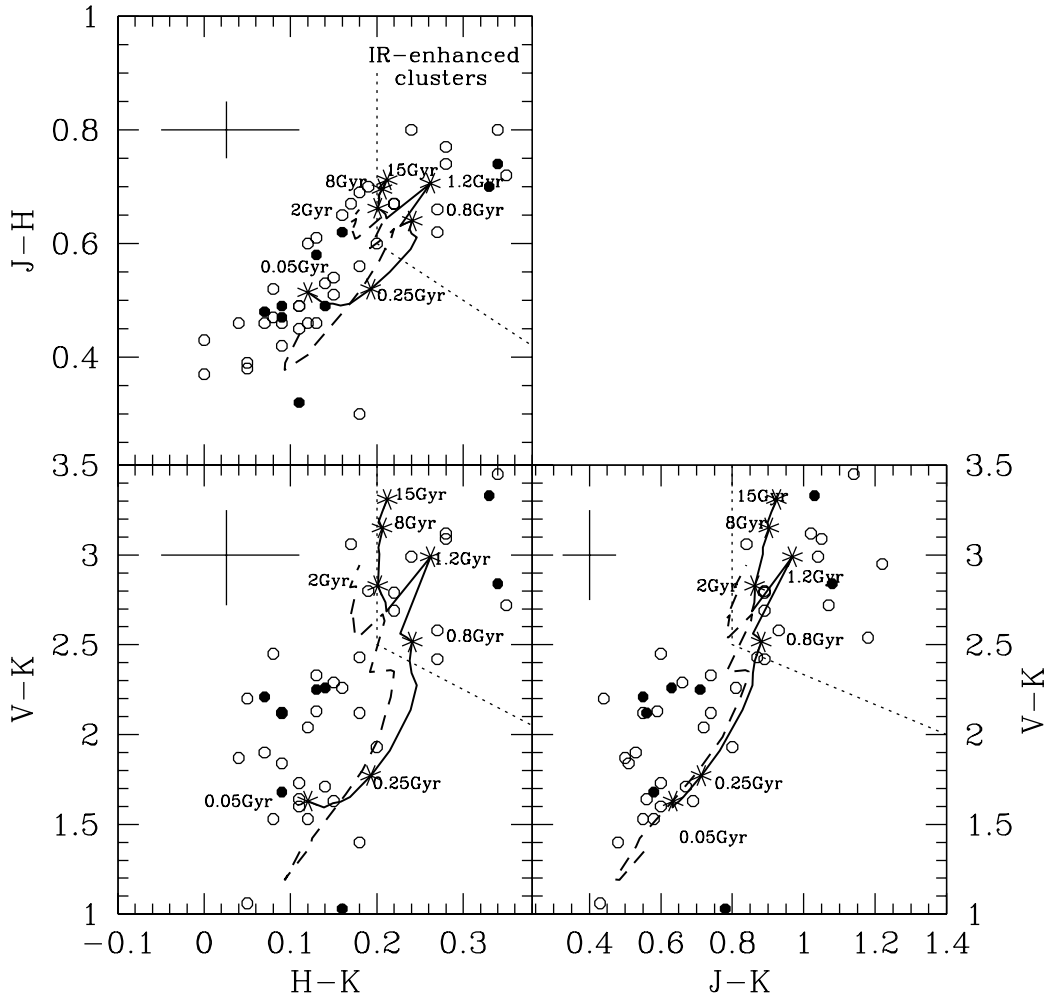

Fig. 16. Comparison of synthetic two-colour diagrams predicted at $Z = 0.008$ and $Z = 0.02$ (continuous and dashed line, respectively) at ages of 0.1–15 Gyr with observed reddening-corrected colours for star clusters in the LMC (open circles) and SMC (filled circles) taken from Persson et al. (1983). Typical error bars are indicated. Also shown are age labels along the solar model track. The *IR enhanced* clusters of Persson et al. (1983) have red colours and a specific range of ages (mean SWB type IV). Those objects are reproduced by stellar populations dominated by AGB stars.

grids of models assuming two stellar spectral libraries differing in the assumed effective temperature scales. The first one is theoretical, and taken from Bessell et al. (1989; as described in Paper II). The authors have considered only static M stars, but with extended atmospheres meant to be appropriate for AGB stars. The second scale was proposed by Feast (1996), based on angular diameter measurements for late-type stars combining Miras and non-Mira M-type stars. A caveat of that scale is the scatter in the empirical data it is based on. All model result previously discussed in the present paper are based on the scale of Bessell et al. (1989).

Models that assume the scale of Bessell et al. (1989) predict deeper molecular bands than those based on the scale of Feast (1996). This follows from the steeper slope of Feast's relation, at the low temperatures relevant to TP-AGB stars: late type stellar spectra with deep molecular bands are assigned higher temperatures, and hence are used much more, in the models with the scale of Bessell et al. than in those with Feast's scale. The resulting changes in the molecular indices are illustrated in Fig. 18. At solar metallicity, oxygen-rich TP-AGB stars, although mixed with carbon stars, contribute significantly to the light, and the temperature scale of the M type spectra is essential. Here, our assumption that all TP-AGB stars are variable also has effects. Using static star spectra rather than LPV spectra during a reasonable first part of the TP-AGB would reduce the oxide features slightly. At $Z = 0.008$ on the other hand, the predominance of carbon stars is such that changes in the temperature scale of the M type spectra are negligible.

The comparison of the new set of theoretical predictions with those of Lançon et al. (1999) again shows the important effects of the stellar evolution inputs on the predicted integrated properties of intermediate-age stellar populations. Lançon et al. (1999) used the stellar evolutionary tracks provided with the Pégase evolutionary synthesis package (Fioc & Rocca-Volmerange 1997). For early evolutionary phases they are identical to the ones used here, but their TP-AGB phase is based on the prescriptions of Groenewegen & de Jong (1993) which, in particular, are incomplete for envelope burning. The main resulting discrepancy between the two sets of models is in the age at which the AGB signatures are the strongest: without

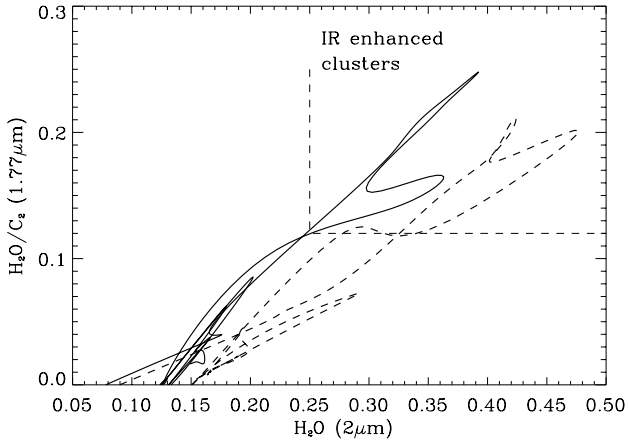

Fig. 17. Synthetic evolution in the prefered two-index diagram. Solid: $Z = 0.008$; dot-dashed: $Z = 0.02$. The upper right corner of this diagram is occupied by stellar populations dominated by AGB stars. They correspond to the IR enhanced clusters as defined by Persson et al. (1983).

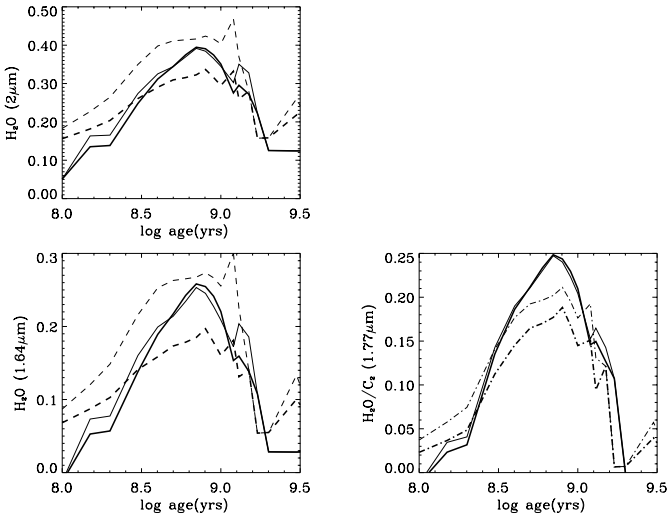

Fig. 18. The time evolution of selected photometric indices that identify AGB stars in single post-starburst populations. Solid curves: $Z = 0.008$, and dashed line to $Z = 0.02$. Thin lines refer to models based on the $T_{\rm eff}$ scale of Bessell et al. (1989), thick lines to those based on the scale of Feast (1996).

envelope burning, this happens much earlier, i.e. at ≈0.2 Gyr, against ≈0.8–0.1 Gyr in the present models. An abrupt transition to red colours and deep molecular features was present around 0.2 Gyr of age, that has now turned into a gradual change. In addition, Lançon et al. (1999) had considered the formation of carbon stars quantitatively only at $Z = 0.008$.

The more extensive grid that we have now computed highlights the sensitivity of the molecular indices to uncertain model parameters. For instance, Fig. 18 shows that it may depend on the adopted effective temperature scales whether photometric indices that were designed to measure H_2O absorption take larger or smaller values in low metallicity systems than at solar metallicity. More data is clearly necessary for the calibration of the models. To avoid the stochastic fluctuations, single stellar populations more massive than the clusters of the Magellanic Clouds should be searched for. Unfortunately, such objects are rare at observable distances. One is cluster number 3 in the merger NGC 7252, a ∼300 Myr old, 10^7 $M_\odot$ candidate. Results from the analysis of the near-IR spectrum of this cluster will be presented by Mouhcine et al. (2002). It would be extremely useful to extend those fundamental observations to a sample with a *range* of intermediate-ages, known for example from optical spectroscopy.

5. Conclusions

In this paper we modelled the spectrophotometric properties of intermediate-age stellar populations, focusing on near-infrared wavelengths. TP-AGB stars were included using a large grid of synthetic evolutionary tracks where the effects of envelope burning and the formation of carbon stars were accounted for in a consistent way, using analytical expressions to take into account all the relevant physical processes. Spectral features of luminous AGB stars were included in the models via the new purpose-designed spectral library of Paper II, which includes spectra for both oxygen-rich and carbon-rich stars.

We have compared our theoretical predictions with observational data from the literature. First, our stellar evolutionary tracks are able to reproduce the observational properties relative to single AGB stars that may affect their contribution to integrated properties of stellar populations (initial mass-final mass relation, period-luminosity relation). The predicted contributions of bright AGB stars and carbon stars to the integrated bolometric luminosity and to the integrated K band luminosity of a single-burst population are close to what is observed in the samples of Magellanic Cloud clusters by Frogel et al. (1990) and Ferraro et al. (1995). In particular, the range of ages at which these contributions are maximal is explained. The contribution of bright AGB stars to the bolometric luminosity is shown not to be a strong function of metallicity, while the contribution of carbon stars increases with decreasing metallicity.

The inclusion of envelope burning, the superwind regime at the tip of the AGB phase, and the third dredge-up events in stellar evolution models are shown to be important in order to match the observational constraints. More specifically, we have confirmed that the evolution of broad-band optical/near-IR colours are heavily affected by the envelope burning from about 0.1 Gyr to ∼1 Gyr, making the colour jump to the red, due to the presence of intermediate-mass stars, more gradual and smoothed than suggested in early models. We showed also that the inclusion of carbon stars in the models makes colours redder than models that consider only oxygen-rich stars. The difference between models with and without carbon stars is an increasing function of metallicity, reflecting the higher carbon star formation efficiency at lower metallicity. Our instantaneous burst models are able to reproduce well the broad-band $VJHK$ colours of a sample of Magellanic Cloud clusters with ages older than 0.1 Gyr. The effects of envelope burning and of carbon stars on the properties of intermediate-age population are important in describing a realistic colour evolution of stellar systems, in particular the many nearby dwarf galaxies with subsolar metallicities.

We have also re-investigated the evolution of selected narrow-band indices (Lançon et al. 1999) that are specifically sensitive to the near-IR spectra of AGB stars, with the aim of using them to search for post-starburst stellar populations. Here again, the effects of envelope burning and of the formation of carbon stars are large. In principle, TP-AGB stars can indeed be identified in the integrated light of intermediate-age stellar populations; and the combination of at least two molecular indices can, at a range of ages, be used to determine whether oxygen-rich or carbon-rich stars are predominant, thus providing useful information on the metallicity of the environment of which the stars were born. However, excellent photometric quality is necessary for such purposes, and the use of spectroscopy remains preferable (a broad spectral coverage should be sought). In addition, the predictions are rather sensitive to model parameters. The effective temperature scale of upper AGB stars remains an important source of uncertainties, and we note that an a posteriori empirical calibration of this scale remains essential. A first step in this direction, based on the most massive star cluster of the merger remnant NGC 7252, will be presented in a companion paper.

Acknowledgements. We would like to thank the referee Dr. J. Harris for careful reading of the paper and his constructive report.

References

Arimoto, N., & Bica, E. 1989, A&A, 222, 89
Barthès, D., & Luri, X. 2001, A&A, 365, 519
Baschek, B., Scholz, M., & Wehrse, R. 1991, A&A, 246, 374
Baud, B., & Habing, H. J. 1983, A&A, 127, 73
Bedijn, P. J. 1987, A&A, 186, 136
Bertelli, G., Bressan, A., Chiosi, C., Fagotto, F., & Nasi, E. 1994, A&AS, 106, 275
Bessell, M. S., & Brett, J. M. 1988, PASP, 100, 1134
Bessell, M. S., Brett, J. M., Wood, P. R., & Scholz, M. 1989, A&AS, 77, 1
Bessell, M. S. 1990, PASP, 102, 1181
Blöcker, T., & Schönberner, D. 1991, A&A, 244 L43
Blöcker, T. 1995, A&A, 297, 727
Blöcker, T. 1999, in The Asymptotic Giant Branch Stars, ed. T. Le Bertre, A. Lèbre, & C. Waelkens, IAU Symp., 191
Boothroyd, A. I., & Sackmann, I.-J. 1988a, ApJ, 328, 653
Boothroyd, A. I., & Sackmann, I.-J. 1988b, ApJ, 328, 671
Boothroyd, A. I., & Sackmann, I.-J. 1992, ApJ, 393, L21
Boothroyd, A. I., Sackmann, I.-J., & Wasserburg, G. J. 1995, ApJ, 442, L21
Bowen, G. H. 1988, ApJ, 329, 299
Bowen, G. H., & Willson, L. A. 1991, ApJ, 375, L53
Bressan, A., Fagotto, F., Bertelli, G., & Chiosi, C. 1994a, A&AS, 100, 647
Bressan, A., Chiosi, C., & Fagotto, F. 1994b, ApJS, 94, 63
Bressan, A., Granato, G. L., & Silva, L. 1998, A&A, 332, 135
Bruzual, A. G., & Charlot, S. 1993, ApJ, 405, 538
Bruzual, A. G. 2002, in Extragalactic Star Clusters, IAU Symp. 207, in press [astro-ph/0110245]
Bryan, G. L., Volk, K., & Kwok, S. 1990, ApJ, 365, 301
Charlot, S., & Bruzual, A. G. 1991, ApJ, 367, 126
Chiosi, C., Vallenari, A., & Bressan, A. 1997, A&AS, 121, 301
Clayton, D. 1983, Principles of Stellar Evolution and Nucleosynthesis, second edition (University of Chicago Press, Chicago)
Da Costa, G. S., & Hatzidimitriou, D. 1998, AJ, 115, 1934
Dreiling, L. A., & Bell, R. A. 1980, ApJ, 241, 736
Fagotto, F., Bressan, A., Bertelli, G. & Chiosi, C. 1994, A&AS, 105, 29
Feast, M. W. 1996, MNRAS, 278, 11
Ferraro, F., Fusi Pecci, F., Test, V., et al. 1995, MNRAS, 272, 391
Fioc, M., & Rocca-Volmerange, B. 1997, A&A, 326, 950
Forestini, M., & Charbonnel, C. 1997, A&AS, 123, 241
Fowler, W. A., Caughlan, G. R., & Zimmerman, B. A. 1975, ARA&A, 13, 69
Frogel, J. A., Mould, J. R., & Blonco, V. M. 1990, ApJ, 352, 96
Frost, C. A., Cannon, R. C., Lattanzio, J. C., Wood, P. R., & Forestini, M. 1998, A&A, 332, L17
Girardi, L., & Bertelli, G. 1998, MNRAS, 300, 533
Girardi, L., Chiosi, C., Bertelli, G., & Bressan, A. 1995, A&A, 298, 87
Girardi, L., Bressan, A., Bertelli, G., & Chiosi, C. 2000, A&AS, 141, 371
Groenewegen, M. A. T., & de Jong, T. 1993, A&A, 267, 410
Groenewegen, M. A. T., & de Jong, T. 1994, A&A, 283, 463
Groenewegen, M. A. T., van den Hoek, L. B., & de Jong, T. 1995, A&A, 293, 381
Habing, H. J. 1996, A&AR, 7, 97
Herwig, F. 1995, in Stellar Evolution: What Should Be Done, 32nd Liège Int. Astrophys. Coll., ed. A. Noels, D. Fraipont-Caso, M. Gabriel et al., 441
Hughes, S. M. G., & Wood, P. R. 1990, AJ, 99, 784
Iben, I., & Truran, J. W. 1978, ApJ, 220, 980
Iben, I., & Renzini, A. 1983, ARA&A, 21, 27
Iben, I. 1985, QJRAS, 26, 1
Jeffries, R. D. 1997, MNRAS, 288, 585
Lançon, A., Mouhcine, M., Fioc, M., & Silva, D. 1999, A&A, 344, L21
Lançon, A., & Mouhcine, M. 2000, in Massive Stellar Clusters, ed. A. Lançon, & C.M. Boily, ASP Conf. Ser., 211, 34
Lançon, A., & Wood, P. R. 2000, A&AS, 146, 217
Lançon, A., & Mouhcine, M. 2002, A&A, 393, 167 (Paper II)
Lattanzio, J. C. 1987, ApJ, 313, L15
Lejeune, T., Cuisinier, F., & Buser, R. 1998, A&AS, 130, 65
Loidl, R., Lançon, A., & Jørgensen, U. G. 2001 A&A, 371, 1065
Maraston, C. 1998, MNRAS, 300, 872
Marigo, P., Bressan, A., & Chiosi, C. 1996a, A&A, 313, 545
Marigo, P., Girardi, L., & Chiosi, C. 1996b, A&A, 316, L1
Marigo, P. 1998, A&A, 340, 463
Marigo, P., Girardi, L., & Bressan, A. 1999a, A&A, 344, 123
Marigo, P., Girardi, L., Weiss, A., & Groenewegen, M. A. T. 1999b, A&A, 351, 161
Mouhcine, M., & Lançon, A. 2000, in Massive Stellar Clusters, ed. A. Lançon, & C.M. Boily, ASP Conf. Ser., 211, 144
Mouhcine, M., & Lançon, A. 2002, MNRAS, submitted
Mouhcine, M., Lançon, A., Leitherer, C., Silva, D., & Groenewegen, M. A. T. 2002, A&A, 393, 101
Mowlavi, N. 1999, in The Asymptotic Giant Branch Stars, ed. T. Le Bertre, A. Lèbre, & C. Waelkens, IAU Symp., 191
Olszewski, E. W., Schommer, R. A., Suntzeff, N. B., & Harris, H. C. 1991, AJ, 101, 515
Paczyński, B. 1970, Acta Astr., 20, 47
Paczyński, B. 1975, ApJ, 202, 558
Persson, S. E., Aaronson, M., Cohen, J. G., Frogel, J. A., & Matthews, K. 1983, ApJ, 266, 105
Pickles, A. J. 1998, PASP, 110, 863
Reid, N., Tinney, C., & Mould, J. 1990, ApJ, 348, 98
Reimers, D. 1975, in Problems in Stellar Atmospheres and Envelopes, ed. B. Baschek, W. H. Kegel, & G. Traving (Berlin: Springer), 229

Renzini, A., & Voli, M. 1981, A&A, 94, 175
Renzini, A., & Buzzoni, A. 1986, in Spectral Evolution of Galaxies, ed. C. Chiosi, & A. Renzini (Reidel, Dordrecht), 195
Richer, H.,B., Olander, N., & Westerlund, B. E. 1979, ApJ, 230, 724
Santos, Jr. J. F. C., & Frogel, J. A. 1997, ApJ, 479, 764
Scholz, M., & Tsuji, T. 1984, A&A, 130, 11
Schild, H. 1989, MNRAS, 240, 63
Searle, L., Wilkinson, A., & Bagnuolo, W. G. 1980, ApJ, 239, 803
Smith, V. V., Plez, B., Lambert, D. L., & Lubowich, D. A. 1995, ApJ, 441, 735
Tantalo, R., Chiosi, C., Bressan, A., & Fagotto, F. 1996, A&A, 311, 361
Tinsley, B. M. 1980, Fundam. of Cosmic Phys., 5, 287
van Loon, J. Th., Zijlstra, A. A., Whitelock, P. A., et al. 1998, A&A, 329, 169
Vassiliadis, E., & Wood, P. R. 1993, ApJ, 413, 641
Wagenhuber, J., & Weiss, A. 1994, A&A, 290, 807
Wagenhuber, J. 1996, Ph.D. Thesis, TU München
Wagenhuber, J., & Groenewegen, M. A. T. 1998, A&A, 340, 183 (WG98)
Weidemann, V. 2000, A&A, 363, 647
Wood, P. R. 1981, in Physical processes in red giants, Proc. of the Second Workshop, Erice, Italy (September 3–13, 1980) (Dordrecht, D. Reidel Publishing Co.), 135
Wood, P. R. 1990 in From Miras to planetary Nebulae, ed. M.O. Mennessier, & A. Omont (Éditions Frontières, Gif-sur-Yvette), 67
Wood, P. R., Whiteoak, J. B., Hughes, S. M. G., et al. 1992, ApJ, 397, 552
Wood, P. R. 1998, A&A, 338, 592
Wood, P. R., Habing, H. J., & McGregor, P. J. 1998, A&A, 336, 925
Wood, P. R., & the MACHO Collaboration 1999, in The Asymptotic Giant Branch Stars, ed. T. Le Bertre, A. Lèbre, & C. Waelkens, IAU Symp., 191, 151
Zijlstra, A. A. 1999, in The Asymptotic Giant Branch Stars, ed. T. Le Bertre, A. Lèbre, & C. Waelkens, IAU Symp., 191, 551